https://doi.org/10.5194/acp-2022-264
Preprint. Discussion started: 19 April 2022

Atmospheric Chemistry and Physics Discussions

Dynamics of aerosol, humidity, and clouds in air masses travelling over Fennoscandian boreal forests

Meri Räty[1], Larisa Sogacheva[2], Helmi-Marja Keskinen[1*], Veli-Matti Kerminen[1], Tuomo Nieminen[1,3], Tuukka Petäjä[1,4], Ekaterina Ezhova[1], Markku Kulmala[1,4,5]

[1]Institute for Atmospheric and Earth System Research (INAR) / Physics, Faculty of Science, University of Helsinki, Helsinki, Finland
[2]Climate Change Programme, Finnish Meteorological Institute, Helsinki, Finland
[3]Institute for Atmospheric and Earth System Research (INAR) / Forest Sciences, Faculty of Agriculture and Forestry, University of Helsinki, Helsinki, Finland
[4]Joint International Research Laboratory of Atmospheric and Earth System Sciences, School of Atmospheric Sciences, Nanjing University, Nanjing, China
[5]Aerosol and Haze Laboratory, Beijing Advanced Innovation Center for Soft Matter Sciences and Engineering, Beijing University of Chemical Technology (BUCT), Beijing, China
*Current: Independent researcher, Finland

Correspondence to: Meri Räty (meri.raty@helsinki.fi)

Abstract. Boreal forests cover vast areas of land in the high latitudes of the northern hemisphere, which are under amplified climate warming. The interaction between the forests and the atmosphere are known to generate a complex set of feedback processes. One feedback process, potentially producing a cooling effect, is associated with an increased reflectance of clouds due to aerosol-cloud interactions. Here, we investigate the effect that the boreal forest environment can have on cloud-related properties during the growing season. The site investigated was in Hyytiälä, Finland, in a region near the edge of the biome. Air mass back trajectories were the basis of the analysis and were used to determine the time each air mass had spent over land prior to its arrival at the station. This enabled tracking the changes occurring in originally marine air masses as they travelled across the forested land. Only air masses arriving from the north-western sector were investigated, as these areas have a relatively uniform forest cover and relatively little anthropogenic interference. We connected the air mass analysis with comprehensive in-situ and remote-sensing data sets covering up to eleven growing seasons. We found that the properties of air masses with short land transport times, thereby less influenced by the forest, differed from those exposed to the forest environment for a longer period. The latter were associated with higher number concentrations of cloud condensation nuclei and increased water vapour content. Indications of corresponding transformations in the cloud layer were observed from satellite measurements. Lastly, longer transport times over forest seem also to slightly enhance the observed precipitation frequency. Most of the variables showed an increase with an increasing land transport time until approximately 60 hours, after which a balanced state with little variation seemed to have been reached. This appears to be

https://doi.org/10.5194/acp-2022-264
Preprint. Discussion started: 19 April 2022


Atmospheric Chemistry and Physics Discussions

the approximate time scale in which the forest-cloud interactions take effect, and the air masses adjust to the local forest environment.

1 Introduction

Boreal forest is a distinct biome dominated by evergreen trees that extends over an area of approximately 15 million square kilometres throughout the northern mid and high latitudes, representing over a third of Earth's total forest area (Bonan, 2008). As with any biome, the prevailing climate, such as the large seasonal temperature variations, controls the extent and conditions of the forest. Conversely, the boreal forest also influences the climate on both local and global scales through the exchange of energy, carbon, water and through the production of atmospheric aerosol (Bonan, 2008; Spracklen et al., 2008; Kulmala et al., 2004). The constant flow of energy and matter between the atmosphere and forest creates a delicate balance, in which perturbations, such as the current climate change, can bring on a mosaic of complex feedback processes (e.g. Abbott et al., 2016; Arneth et al., 2016; Euskirchen et al., 2010; Keenan et al., 2016; Kulmala et al., 2014, 2020; Paasonen et al., 2013; Prăvălie, 2018). Some of these feedbacks are positive, amplifying the change, while some are negative and act opposite to the initial perturbation.

The high-latitude boreal forests are undergoing amplified warming (Serreze and Barry, 2011). The rising CO_2 levels and changing temperatures cause direct changes in the boreal carbon cycle. For example, CO_2-fertilisation and a likely future northward expansion of the boreal forest can promote the carbon sink in forest biomass (Qian et al., 2010; Bruhwiler et al., 2021). However, simultaneous thawing of permafrost and decomposition of carbon stored in soils could even lead to a net release of carbon in the region (Abbott et al., 2016; Gonzalez-Eguino and Neumann, 2016; Hartley et al., 2012; Schuur et al., 2009) .

Biome shifts also affect the energy balance at the surface. The decreasing snow cover and expansion of shrubs and especially dark forest canopies over a former tundra reduce the amount of radiation reflected at the surface, creating a positive feedback (Betts, 2000; Pearson et al., 2013; Zhang et al., 2013). However, it is possible that the lost reflectance at the surface could be offset by an increased reflectance by clouds (Spracklen et al., 2008; Kulmala et al., 2020; Yli-Juuti et al., 2021; Teuling et al., 2017; Duveiller et al., 2021). This effect is related to changes in atmospheric aerosol particles.

During the growing season, boreal forest is a significant source of biogenic secondary organic aerosol (SOA) into the atmosphere. In this photosynthetically active period, the forest can maintain a loading of aerosol particles in climatically-relevant sizes (<50-100 nm) that is between 1000 and 2000 cm^{-3} (Tunved et al., 2006). Most of the mass in these particles is organic, consisting of condensed low volatility vapours that have been formed through oxidation of biogenic volatile organic compounds (BVOCs) emitted by the vegetation (Heikkinen et al., 2020). The most abundant BVOC group emitted by the boreal trees, monoterpenes (Tarvainen et al., 2007), are comparatively potent at producing low volatility vapours in comparison to some other common BVOCs (Ehn et al., 2014). Concentrations of BVOCs have high seasonal variabilities, as their emissions are largely tied to the photosynthetic activity in plants (Rantala et al., 2015). Emissions of BVOCs also vary

https://doi.org/10.5194/acp-2022-264
Preprint. Discussion started: 19 April 2022


Atmospheric Chemistry and Physics Discussions

in response to environmental stressors (Peñuelas and Staudt, 2010; Loreto and Schnitzler, 2010; Taipale et al., 2021), and for example warm temperatures can significantly increase their emission rate (Tingey et al., 1980; Lappalainen et al., 2009). An important source of SOA-containing particles is atmospheric new particle formation (NPF) (Mäkelä et al., 1997; Tunved et al., 2006; Ehn et al., 2014). Days having a well-defined NPF event vary in frequency over the boreal region, with examples ranging from only 1.5 % at a remote continental site (Wiedensohler et al., 2019), to 23% in the Finnish boreal forest (Nieminen et al., 2014). While not exclusive (Zhang et al., 2021; Kulmala et al., 2017, 2021), a high condensation sinks (CS) can inhibit NPF, especially in clean sites (e.g. Birmili et al., 2003; Hyvönen et al., 2005) where the more pristine sources of air masses are more favourable for NPF (Tunved et al., 2006; Sogacheva et al., 2005, Vana et al., 2016).

Atmospheric aerosol particles influence the radiation balance at the surface directly through scattering and absorption, as well as indirectly through aerosol-cloud interactions. Every cloud droplet in the atmosphere is condensed around an aerosol particle that may vary in size depending on humidity as well as the properties of the condensation nucleus, but typically particles with dry diameters of 50-100 nm or larger (Paasonen et al., 2018; Pruppacher and Klett, 2010; Kerminen et al., 2012) can activate the nucleation of a cloud droplet and are therefore called cloud condensation nuclei (CCN). The number of available CCN affects the number and size of droplets in clouds, with potentiantially great influences on the cloud albedo and lifetime (Twomey, 1977; Christensen et al., 2020). A higher CCN concentration means in practise that the available water can distribute to a larger number of smaller droplets, which leads to more reflective clouds and changes in cloud lifetimes (Twomey, 1977; Christensen et al., 2020).

If CCN concentrations were to increase, the increased reflectance of clouds could lead to a cooling effect (Yli-Juuti et al., 2021). Boreal BVOC emissions are expected to increase in the future with an increase in the amount of photosynthesising biomass, and warmer temperatures, amongst other possible effects (Peñuelas and Staudt, 2010), can further increase the emission rate of BVOCs on an individual plant level (Loreto and Schnitzler, 2010). The increase in BVOCs can then go on to increase the production of SOA and ultimately the number concentrations of CCN (Scott et al., 2014; Paasonen et al., 2013), which can ultimately increase cloud reflectivity and generate a negative feedback under climate change (Sporre et al., 2019).

In addition to providing the nuclei for cloud droplets, the forest also provides the condensing water vapour. While some of the life-sustaining forest rainfall flows back into the oceans through rivers and lakes or is filtered into groundwater, a significant portion is evapotranspired: either evaporated from wet surfaces or transpired by vegetation back into the atmosphere. For example, in a forest site in Sweden, total evapotranspiration during a growing season was estimated to be 85% of precipitation, while 75% of it was estimated to be contributed by trees by means of transpiration and evaporation from the canopy (Kozii et al., 2020). This water vapour expelled by the forest can then be “recycled” and go on to form new clouds and precipitation. Globally, total continental evapotranspired water vapour is a significant source of precipitation, and especially remote continental areas are highly dependent on recycled continental water (van der Ent et al., 2010). Some estimates of the average contribution of the total recycled terrestrial water vapour to the precipitation falling over continents range from 40% (van der Ent et al., 2010) to around 60 % (Schneider et al., 2017), but for example in China, rainfall can be

https://doi.org/10.5194/acp-2022-264
Preprint. Discussion started: 19 April 2022


Atmospheric Chemistry and Physics Discussions

up to 80% recycled from the water vapour air flows have picked up while crossing the Eurasian continent (van der Ent et al., 2010). Forest surface properties also have a role in distributing moisture into the atmosphere. In comparison to open lands, forests absorb more radiation and have a high surface roughness, generating a thicker atmospheric boundary layer that can promote effective uplift for the moisture provided by the surface evapotranspiration (Bosman et al., 2019; Teuling et al., 2017, Xu et al., 2022).

Together, both CCN and the atmospheric moisture provided by the boreal forest can boost the cloud cover in the growing season, increasing reflectance while also providing inland precipitation. Previous findings indeed suggest the boreal forest cover to promote higher levels of cloud fractional cover in comparison to unforested land at least in summer and autumn (Duveiller et al., 2021; Xu et al., 2022), while the opposite could be true for low-level cloud fraction in winter and spring (Duveiller et al., 2021). These outlined interactions between clouds and forests are important considerations for the future, where the area covered by forest might change either naturally, or via human intervention, and the interactions themselves are changing due to the stress of the warming climate. Under the changing climate, existing boreal forests are expected to generate a summertime cooling cloud radiative feedback (Yli-Juuti et al., 2021; Spracklen et al., 2008), but the estimates are still associated with large uncertainties (e.g. Carslaw et al., 2010). As many studies revealing cloud-forest interactions are mainly based on satellite and/or model data, more direct measurements are required to unravel how these interactions fit in the larger framework of other competing feedbacks in the region.

In this manuscript, we aim to capture the large-scale interactions between the boreal forest environment and the atmosphere discussed above, by investigating a comprehensive data set of air mass transport history and connecting land transport times of initially marine air masses over the forest with associated changes occurring in aerosol properties and humidity (following the examples of e.g. Tunved et al., 2006; Liao et al., 2014; Petäjä et al., 2022; Heikkinen et al., 2021). We also investigate how these changes might translate to changes in cloud optical properties and ultimately the amount of precipitation falling back to the surface. We consider air masses with very short transport times over land to be representative of marine air masses, whereas air masses spent longer periods of time over the forested land are expected to show clearer signs of having been influenced by the forest. With this methodology, and through the comparison of the closer-to-marine and the increasingly more terrestrial air masses, we can examine the characteristics of the cycle of interactions outlined here and estimate the temporal scale of these effects through the time scale of the transition of initially marine air masses reaching a continental steady state between sources and sinks of water vapour and aerosol in this environment

2 Methods

Our analysis was based on hourly air mass back trajectories, investigated with coinciding in-situ measurements and remotely sensed variables. The site of the measurements was the SMEAR II station in Hyytiälä (61°51´N, 24°17´E, 170 m asl),

https://doi.org/10.5194/acp-2022-264
Preprint. Discussion started: 19 April 2022


Atmospheric Chemistry and Physics Discussions

located in the Finnish boreal forest (Hari and Kulmala, 2005). The population in the area is sparse and the nearest urban area of significant size is the city of Tampere (pop. 240 000), located approximately 50 km southwest from the site.

We concentrated on observations from an 11-year-long period, 2006-2016, except for CCN data, for which we had measurements from eight years (2009-2016). Only the growing season (April-September) was analysed, as we were specifically interested in investigating the biogenic influences of the forests which are important only when the vegetation is biologically active (e.g. Aalto et al., 2015; Hari et al., 2017). All the data used in our analysis are listed in Table 1.

The hourly air mass back trajectories used in the analysis presented here were modelled with the Hybrid Single-Particle Lagrangian Integrated Trajectory model (HYSPLIT) (Stein et al., 2015; Draxler and Hess, 1998). The trajectories had been routinely produced throughout the years, and the meteorological input was updated whenever a new input was deemed more suitable for the purpose, or the old data were no longer produced. Therefore, several different NCEP meteorological datasets were used to run the model, FNL for 2006, GDAS for 2007-2013 and GFS for 2014-2016 (Table 1). The last one had a horizontal resolution of 0.5°, while in the other two it was 1°. The output frequency of the meteorological data was 3 hours. The trajectory arrival height was set to 100 metres. Each trajectory covered a 96-hour long air mass history with a 1-hour temporal resolution.

We focused our analysis *only* on the air masses arriving from a sector between the west and north. This is the typical sector to focus on when wishing to specifically examine clean air masses arriving at the site (e.g. Tunved et al., 2006; Petäjä et al., 2022). More specifically, we selected trajectories that were 90% or more within the area indicated in Figure 1. As there are no large cities or other substantial pollution sources in this area, we can expect most surface effects on the air mass to be biogenic. Anthropogenic influences can, however, not be fully ruled out as, while relatively sparsely populated, the area does include towns, other built environments and agricultural land.

For the selected "clean sector" trajectories, we calculated the 'Time over Land' (ToL) value. It included the time spent over continental land mass in our chosen area, while any time spent over islands (e.g., Greenland and Iceland) was ignored. Therefore, in practice, ToL refers to time spent over Fennoscandia in this context. The ToL was not necessarily a continuous period on land, as some air masses spent some time over the Baltic Sea in between.

The HYSPLIT trajectories are not perfect in capturing the path of the air mass, with some estimations suggesting 20 % position errors of the travel distance can be fairly common, while errors can vary substantially between individual trajectories (Stohl, 1998). These uncertainties naturally carry over to our air mass classification (by sector) and ToL values. However, as we are not focusing on individual trajectory paths, but only on the general source region and an approximate characterisation of the path in the form of ToL, in addition to investigating a very long and extensive dataset, we expect a reasonable ratio between reliable signal and inaccuracies in individual trajectories.

As roughly 75% of the land area of Finland and Sweden, as well as above 45% of the land area of Norway are covered by forests or other wooded land (European Commission, 2021), we consider ToL a sufficient proxy, in the range of our other uncertainties at least, for describing the time an air mass is influenced by a forest environment. A more detailed forest distribution in the area is shown in the map in Figure 1.

https://doi.org/10.5194/acp-2022-264
Preprint. Discussion started: 19 April 2022

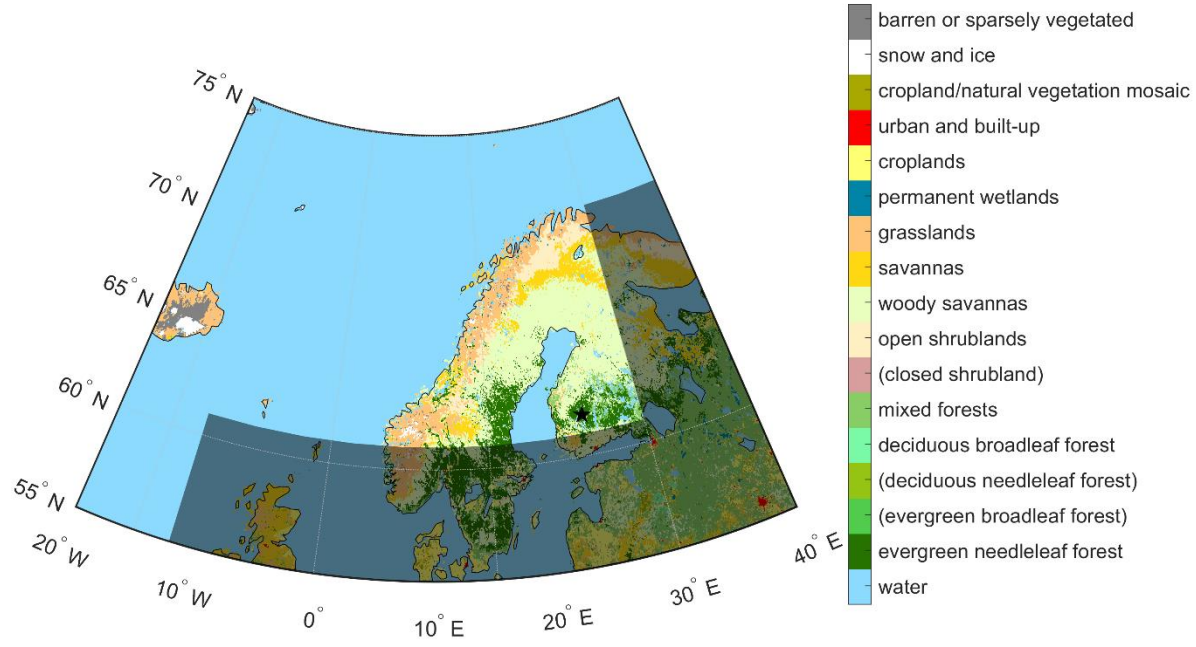

Figure 1. Map indicating the "clean sector" (not shaded). Only trajectories spending 90% or more within the clean sector were included in the analysis. Shown 2011 majority land cover types are from MODIS Terra and Aqua MCD12C1 data product (Friedl and Sulla-Menashe, 2015), and follow the International Geosphere–Biosphere Programme (IGBP) land cover classification system (Loveland and Belward, 1997; Belward et al., 1999). The classes in brackets are not present in the area. (The classification system's labelling of most of the Nordic boreal forest as "woody savanna" could be an artefact rather than the area truly meeting the set criterion of the class, as it is the class evergreen needleleaf forest pixels are the second most likely to switch to between years (Broxton et al., 2014).)

To investigate differences in air masses with different ToLs, routinely measured meteorological datasets from Hyytiälä (temperature (T), relative humidity (RH), pressure (P) and dew point temperature T_d) were used. Specific humidity (q) was the only parameter not directly measured but it was derived from measured P and T_d (following formulations provided by WMO, 2018). Original 10-minute resolution data were converted to 1-hour resolution by taking hourly medians. Precipitation was only considered in terms of accumulation within the next 1 to 3 hours after the arrival of an air mass, which was similarly a sum of initial 10-minute accumulation data. When a multi-hour rainfall was investigated, only periods in which the source region remained within the clean sector were accepted.

The CCN data used in this analysis were from a Cloud Condensation Nuclei Counter (CCNC, CCN-100, Droplet Measurement Technologies) measurements. The CCNC is a multicomponent setup that, in addition to the main chamber, also includes a Condensation Particle Counter (CPC) that measures the total aerosol number concentration in the sample (N_{CN}), and an Optical Particle Counter that resolves the number concentration of particles activated in the chamber (N_{CCN}). More detailed descriptions of the instrument and measurements can be found in literature (Paramonov et al., 2015; Roberts

https://doi.org/10.5194/acp-2022-264
Preprint. Discussion started: 19 April 2022


Atmospheric Chemistry and Physics Discussions

and Nenes, 2005; Rose et al., 2008; Schmale et al., 2017). Different-size particles are activated into CCN by varying the supersaturation (S_{eff}) in the chamber. In this analysis, we examine measurements conducted at supersaturations of 0.2 and 0.5 %. The measurements were not uniformly distributed between the years, as the supersaturation settings and measurement frequency varied between the years (Table 1). More details on the data availability of CCN measurements at the supersaturations investigated in this work are shown in Table 1. In addition to CCN measurements, we utilised aerosol number size distribution and number concentration measurements made with the Differential Mobility Particle Sizer (DMPS) setup (Aalto et al. 2001).

Remotely sensed parameters, cloud optical thickness (COT), cloud fraction (CF), and cloud water path (CWP), were acquired from the MODIS Level-2 Cloud Product (Platnick et al., 2017), based on the retrievals by the satellites MODIS Terra and Aqua. Only the main COT and CWP datasets were used (variables *Cloud_Optical_Thickness* and *Cloud_Water_Path*), which include observations only from pixels expected to be overcast (Platnick et al., 2018). All COT and CWP observations that were within the valid range (i.e., not fill values) were included (including zeroes), and no additional weighing, selection or cleaning for the pixels were implemented. Therefore, pixels with any of the cloud phase flags (liquid, ice, undetermined) leading to processing were also included. CF (*Cloud_Fraction*), which is based on the fraction of 1km-resolution pixels flagged with a cloud mask (of "probably cloudy" or "confident cloudy") (Platnick et al., 2018), was similarly used without additional filtering. We took medians and means from the satellite pixels from an area of 1 longitudinal and 0.5 latitudinal degrees, with Hyytiälä in the centre. At this latitude, such area corresponds to approximately 52-53 km and 55.6 km in zonal and meridional distance, respectively. Some satellite views over the area are partial and cloud optical properties are only retrieved for cloudy pixels, meaning that an average over the satellite view of the pixels in the defined area could at worst be based on only a few pixel observations. Therefore, we defined a threshold, in which the averages calculated had to be based on a number of pixels at least 20% of the observed maximum pixel coverage. For CF, this in practice means that the satellite view had to cover at least 20% of the 1° × 0.5° grid, whereas for COT and CWP which are only derived for overcast cloudy pixels, this could be either a similar partial view, or even a full view but with overcast cloud pixel coverage 20% of the observed maximum.

A minor fraction of satellite data was lost in file-by-file processing, leading to the rejection of some partial views where files happened to be "cut" over the region, and a few sporadic observations outside the main time window (8-12 UTC, 10-14 EET) were also discarded. To match the satellite averages with the hourly trajectories, we applied rounding to the nearest hour, and when there were several satellite overpasses within the same hour, we took an average weighed with the number of pixels that went into calculating the averages from the single satellite views.

In most of our analysis, we divided observations into four value ranges and compare the fraction of cases in each bin in air masses with varying ToL. The variance in these complex natural variables is significant, but by this method, it is easy to observe the changes in the fraction of cases belonging to the higher or lower value ranges. As in many of our figures the data is divided into 5-hour ToL bins, we use 92.5 hours as a cut-off limit for ToL. The next bin would not be a full 5-hour bin and in the event of full trajectories (96 h) being located over land, accurate determination of total ToL is not possible as it can

https://doi.org/10.5194/acp-2022-264
Preprint. Discussion started: 19 April 2022

Atmospheric Chemistry and Physics Discussions

then be longer than the trajectory length. For consistency, this same cut-off is also used when data binned hourly. Bins of the shortest ToLs that had only 5 or less data points were also omitted.

225

Table 1. A summary of the datasets used in this study. The meteorological inputs for the HYSPLIT simulations were from the U.S. National Oceanic and Atmospheric Administration's (NOAA) Air Resources Laboratory's (ARL) archives of the National Centers for Environmental Prediction (NCEP) meteorological model data. This included data from the FNL archive, and two Global Data Assimilation System (GDAS) archives (freely available on their website). Satellite observations were averaged over a 1°x0.5° geographical grid, which at this location corresponds to approximately 53 km x 56 km. The numbers in brackets in "Availability" indicate variation between years.

230

Dataset	Temporal coverage (Apr-Sep)	Availability (%) in clean sector air masses	Hourly resolution achieved	Additional	Reference
HYSPLIT 96-hour back trajectories	2006-2016		Modelled hourly		Stein et al., 2015; Draxler and Hess, 1998; (available at: https://www.ready.noaa.gov/HYSPLIT_linux.php)
	2006			Meteorological input: 1°, NCEP/FNL	(available at: https://www.ready.noaa.gov/archives.php)
	2007-2013			Met input: 1°, NCEP/GDAS	
	2014-2016			Met input: 0.5°, NCEP/GDAS	
Condensation Nuclei (N_{CN})	2009-2016	85%	Hourly median	Instrument: CCN-100	Paramonov et al., 2015; Roberts and Nenes, 2005; Rose et al., 2008; Schmale et al., 2017
Cloud Condensation Nuclei (N_{CCN})	2009-2016		Rounding to nearest hour (or average if multiple)	Instrument: CCN-100	"
		57% (35-73%)		at S_{eff}=0.2	
		33% (0-63%)		at S_{eff}=0.5	

https://doi.org/10.5194/acp-2022-264
Preprint. Discussion started: 19 April 2022

Aerosol number size distribution	2006-2016	99%	measurement at time of trajectory arrival	Instrument: DMPS	Aalto et al. 2001
In-situ meteorological parameters (T, RH, q, P)	2006-2016	95-100%	Hourly median for others, accumulation in the next hour for precipitation	Tower measurements (T, RH, q) at 16.8 m and weather sensor at 18 m (P)	available at: https://smear.avaa.csc.fi/; q derived from P and T_d (following equations by WMO, 2018)
Cloud optical thickness (COT)	2006-2016	5%	Rounding (pixel-weighted average if multiple observations)	MODIS Terra & Aqua Mean or median in 1°x0.5° geographical grid with minimum 20% data coverage	Platnick et al., 2017
Cloud water path (CWP)	2006-2016	5%	Rounding (pixel-weighted average if multiple observations)	MODIS Terra & Aqua Mean or median in 1°x0.5° geographical grid with minimum 20% data coverage	"
Cloud Fraction (CF)	2006-2016	11%	Rounding (pixel-weighted average if multiple observations)	MODIS Terra & Aqua Mean or median in 1°x0.5° geographical grid with minimum 20% data coverage	"

235

https://doi.org/10.5194/acp-2022-264
Preprint. Discussion started: 19 April 2022

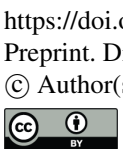

Atmospheric Chemistry and Physics Discussions

3 Results and Discussion

During the approximate growing season of April to September in the 11 years of observations considered here, 27% of trajectories came from the clean sector. For these trajectories, the mean and median ToL were 38 and 33 hours, respectively, and the mode of ToL rounded to the nearest 5 hours was 25 hours. The average monthly distribution of ToL is shown in Figure 2. In April and September, the median ToL between all the years considered were only 28 and 31 hours, while in August it was exceptionally long (44 hours) in comparison to the rest of the months. Clean sector trajectories were, however, also notably rarer in August.

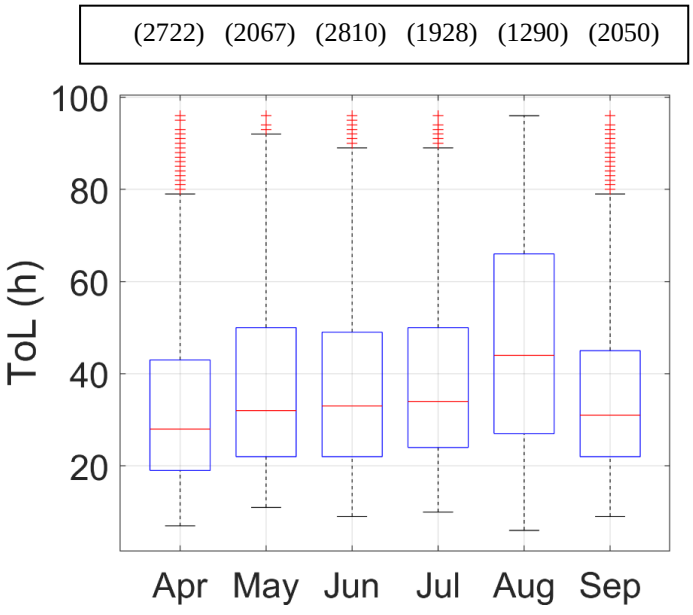

Figure 2. Monthly (growing season) distribution of ToL in air masses arriving from the clean sector in 2006-2016. The red bars show the median of the observations, while the top and the bottom of the boxes indicate the 75th and 25th percentiles. The whiskers mark the furthest observations that are not classified as outliers, which are indicated with the red crosses and are more than 1.5 times the interquartile range away from the box limits. The number of clean sector trajectories in each month in the 11 years is shown in the text box above.

3.1 Aerosol particles as a function of Time over Land

In Figure 3, arriving air masses are divided into 4 groups based on their aerosol particle number concentration (measured with the CCNC and therefore herein also referenced as number concentration of condensation nuclei, N_{CN}). The fraction of air masses belonging to each value group changes with ToL. In air masses with the shortest ToLs of approximately 10 hours, condensation nuclei concentrations are mostly low: nearly half of them have number concentrations below 1400 cm^{-3}, and more than 60% below 2200 cm^{-3}. Air masses with slightly longer ToLs tend to have much higher N_{CN}. Less than 15% of air masses that spent 20 hours over land had number concentrations below 1400 cm^{-3}. Nearly 45% of them on the other hand,

https://doi.org/10.5194/acp-2022-264
Preprint. Discussion started: 19 April 2022

Atmospheric Chemistry and Physics Discussions

belonged to the high concentration group, with number concentrations exceeding 3400 cm^{-3}. The high abundance of particles at these relatively short continental transport times is likely a result of the very high occurrence rate of NPF events in such air masses (Petäjä et al., 2022).

It appears that in a relatively short exposure (15-20 h) to the forest, an originally marine air mass accumulates BVOC concentrations and subsequent oxidation products that promote NPF (Tunved et al., 2006). Why the characteristic total number concentration is lower at the shortest 10 hours of ToL could be explained by lower BVOC accumulation, but also by NPF inhibition due to cloudiness, as these fast-moving air masses are more likely to be associated with cloudy frontal activity. When ToL increases beyond the point where highest number concentrations were observed, the air masses are more likely to have already undergone NPF, and thus available condensable vapours are more likely to partition into pre-existing particles, so that the probability for NPF is decreased. At the same time, existing particles s are subjected to sinks like coagulation or deposition. Correspondingly, we observe that the probability for high number concentrations decreases between 20 and 60 hours of ToL, concentrations above 2200 cm^{-3} for example dropping from the peak value of 70% to only around a third of cases. After 60 hours over land, the fraction of cases in each value group becomes relatively stable, exhibiting only modest fluctuations. This stabilization after 60 hours suggests this to be the approximate time scale in which the air mass transitions from marine to continental, reaching a balanced state with the forest environment.

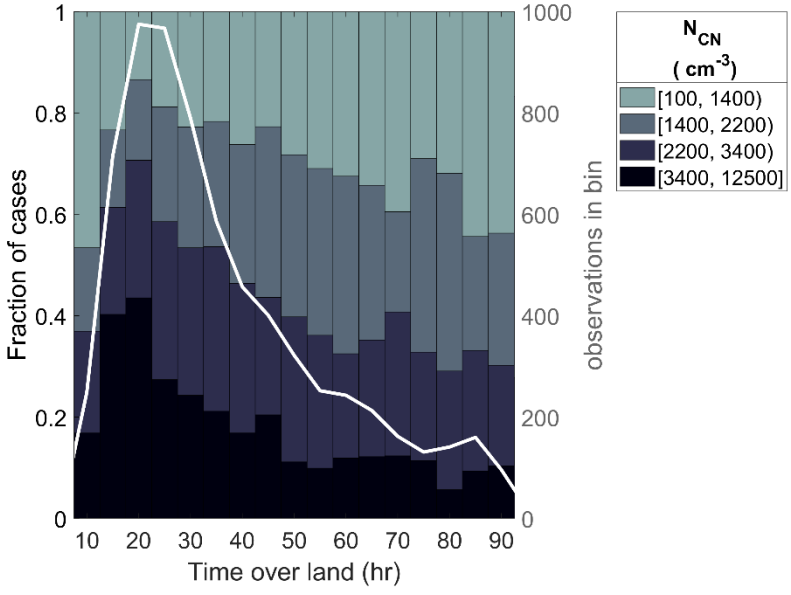

Figure 3. Fractions of measured condensation nuclei (N_{CN}) number concentrations in 4 different value groups in air masses divided into 5-hour Time over Land bins. The white line and the right y-axis show the number of observations in each bin. Six outliers more than 6 mean absolute deviations (MAD) from the mean were excluded (between 12500 and 19000 cm^{-3}). The ranges are based on data percentiles, the value group roughly representing the 0^{th}-25^{th}, 25^{th}-50^{th}, 50^{th}-75^{th} and the 75^{th}-100^{th} percentiles.

The median aerosol number size distributions in air masses with different ToL (Figure 4) resembles the evolution of aerosol number size distribution during a regional NPF event (Dal Maso et al., 2005). Similar aerosol processes that take place

https://doi.org/10.5194/acp-2022-264
Preprint. Discussion started: 19 April 2022

Atmospheric Chemistry and Physics Discussions

during the formation and growth of particles in a single location during an event, seem to vary in prevalence and determine the average aerosol population in air masses with increasing times of exposure to the boreal forest. In Figure 4 we can see how, as a consequence of the prevalence of NPF events at short ToLs, these air masses are typically characterised by particles that are small in size and large in numbers. After 20 hours, the increase in ToL is accompanied by lower number concentrations and larger particle sizes, until a seemingly balanced is reached when ToL exceeds approximately 60 hours. Before such balancing, the peak of the median size distributions shifts from approximately 22 nm to 72 nm between the 10-hour and 60-hour ToL bins, corresponding to a rate of change of roughly 1nm per h of ToL.

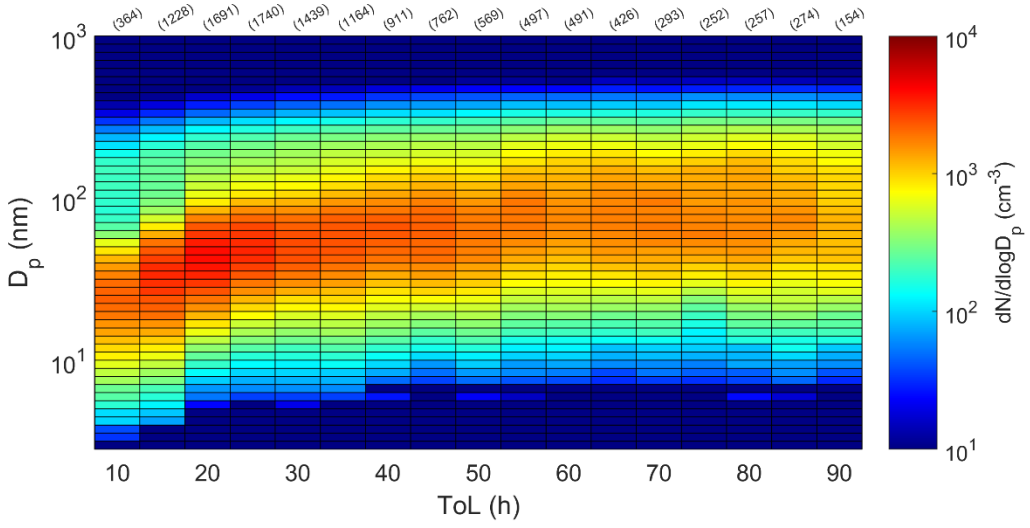

Figure 4. Median aerosol number size distribution in air masses with different ToL. The numbers in top show the number of trajectories in each bin.

While Figure 4 shows the growth and shift of particle size distributions towards larger sizes between 10 and 60 h ToLs, from Figure 5 we can see a corresponding increase in measured CCN concentrations. We analysed CCN measurements at two supersaturations, 0.2% and 0.5%. In Hyytiälä, the median (non-normalised method) critical diameters at these supersaturations are 96 and 67 nm, respectively (Paramonov et al., 2013; the latter value estimated from the values provided therein). In clouds, peak supersaturations vary greatly depending on the aerosol load and meteorological conditions like the updraft velocity. For example, if the air is polluted, effective supersaturation in a stratus cloud may be approximately 0.1%, while in clean maritime air mass it can regularly exceed even 1% (Hudson and Noble, 2014). In Hyytiälä, 0.2% supersaturation in clouds can be expected to be quite common, while 0.5% might require high vertical velocities and a relatively low numbers of CCN (Pruppacher and Klett, 2010; Pinsky et al., 2014; Väisänen et al., 2016).

The differences in CCN concentrations between the air masses with different land travel times are notable. At the supersaturation of 0.2% for example, when ToL is 10 hours, 30% of air masses have N_{CCN} that are above 110 cm^{-3}. After 60 hours of ToL, this covers around 95% of cases, while around 85% have number concentrations higher than 180 cm^{-3} and nearly 60% have number concentrations between 300 cm^{-3} and 1660 cm^{-3}. The increased probability of high CCN number

https://doi.org/10.5194/acp-2022-264
Preprint. Discussion started: 19 April 2022

Atmospheric Chemistry and Physics Discussions

concentration is observed again up about 60 hours of ToL, after which the probability for specific CCN ranges appear to less influenced by ToL. A similar development is seen in measurements at 0.5% supersaturation, with higher particle numbers due to the wider size range of particles being activated. Examining Figures 5 b and d clearly shows that the increase in CCN concentrations originates from the increased N_{CCN} to N_{CN} ratio (Figure 5 b and d). Particles grow in size while travelling in the forest environment, and consequently more and more of them enter the CCN size ranges. Earlier investigations have also similarly connected ToL to increasing aerosol mass, both in the same location (Tunved et al., 2006; Petäjä et al., 2022), as well as in a coastal arctic Siberian site (Asmi et al., 2016).

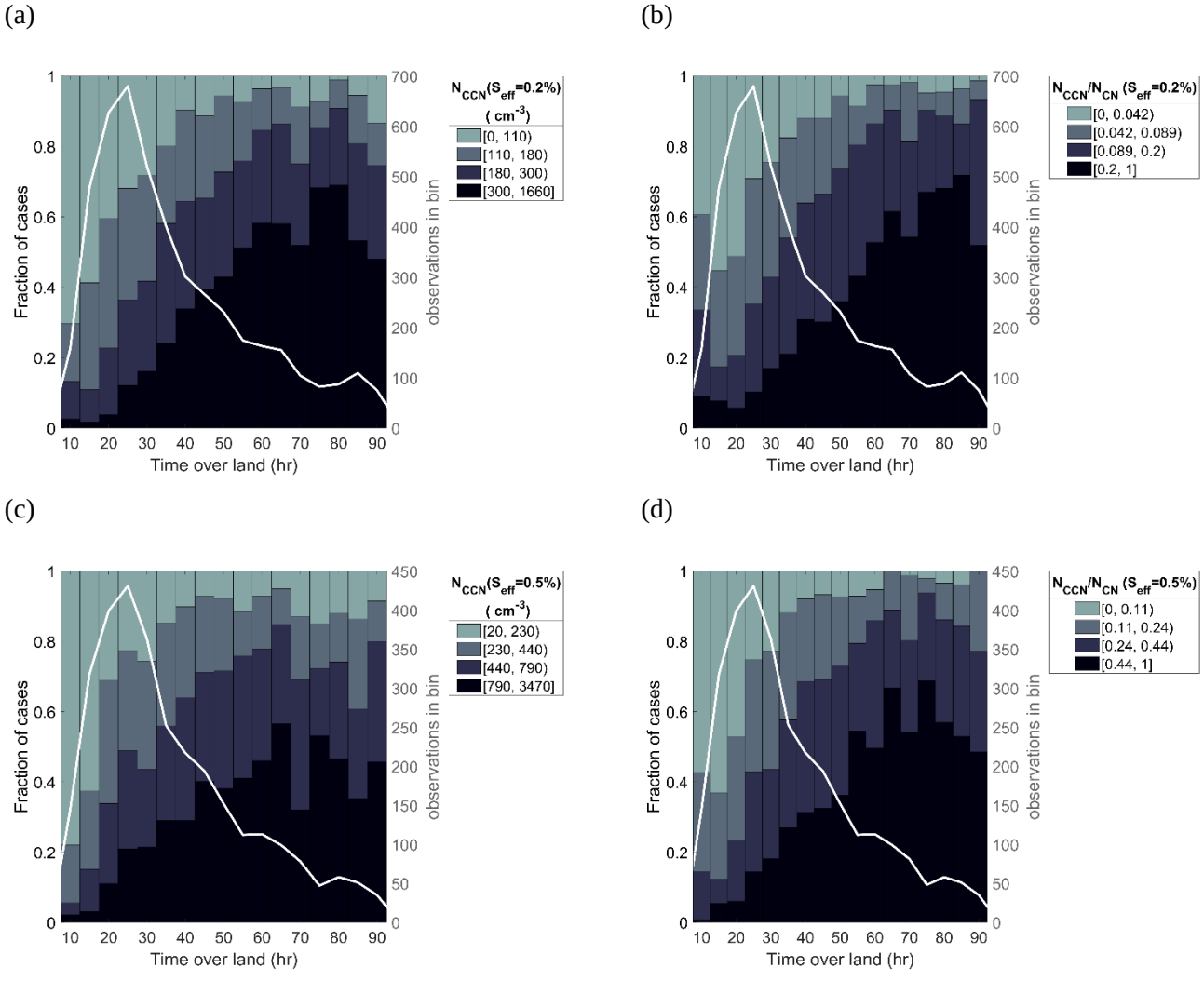

Figure 5. Fractions of observed (a) N_{CCN} and (b) $N_{CCN/CN}$ ratio at 0.2% supersaturation, and (c and d) at 0.5% supersaturation in 4 different value ranges, as a function of ToL. The white line and the right y-axis show the number of observations in each bin. The general description of this figure is the same as for Figure 3. Fourteen and five outliers (MAD>6) were excluded from figures (a) (1700-3900 cm^{-3}) and (c) (4300-7200 cm^{-3}) respectively.

https://doi.org/10.5194/acp-2022-264
Preprint. Discussion started: 19 April 2022


Atmospheric Chemistry and Physics Discussions

3.2 Atmospheric humidity as a function of Time over Land

Air masses with longer ToL tend to contain more water vapour (Figure 6a). While high specific humidities (q), between 6.3 and 13 g/kg are nearly non-existent at the shortest ToLs, they constitute around 40% of the air masses with ToL exceeding 60 hours. Conversely, very dry air masses (0-3.5 g/kg) account for approximately 40% of the observations when ToL is very short (15 hours) but are less common (~15%) when ToL is longer. These differences in specific humidities are at least in part explained by the temperature differences between these air masses (Figure 6b). In Figure 7, simultaneous observations of specific humidity and temperature form a clear upper boundary corresponding to the saturation specific humidity. This figure illustrates how, for example, specific humidities that are above 6.3 g/kg (i.e. minimum of the largest value group) are only possible when temperatures are above 6.6°C. More than 65% of air masses with very short ToLs of 10 hours and less are colder than this (not shown). Typical air mass temperatures vary drastically with short ToLs, and when ToL reaches 15 hours, already more than 30% of air masses are warmer than 9.8°C. When ToL is above roughly 45 hours, air masses within the different temperature ranges already seem relatively constant, and approximately 80%, 60% and 35% exceed temperatures 5.5°C, 9.8°C and 14°C, respectively.

In summer, we expect the air masses to warm up as they travel over land, as more energy partitions into sensible heat flux over the continent than over the ocean (Wild et al., 2015). Our studied season, however, covers half a year, so the temperature variation is significant also from seasonal effects alone, which might interfere with separating the effect of the land transport from possible seasonal differences in typical atmospheric flow. The shorter-than-average ToL in April and September might in part explain why short ToLs were more often observed alongside colder temperatures, while incidentally during the much warmer months of August the average ToLs happened to be also longer (Figure 2). We also compared the individual temperatures to the monthly median (of all air masses from all directions) temperatures of the 11 years (Figure 6c), which provided further indication on the warming of air masses being associated with longer travel times over land. After the local minimum at 17-hour ToL, where roughly 75% of air masses were colder than average, the fraction of warmer air masses increases with ToL. Finally, after approximately 60 hours, there were approximately the same amount of warmer-than-average, as there were colder-than-average air masses. Considering that the maximum specific humidity at 17°C is almost three times that at 1°C (Figure 7), the role of temperature in enabling the accumulation of moisture is undeniable, even though the scatter between temperature and humidity can be quite high. The water itself is likely to originate from forest evapotranspiration (Hornberger et al., 2014), and our observations underlines the importance of forests as a water source. In line with our hypothesis of increasing specific humidity being mostly facilitated by warming, no clear trend is seen between relative humidity (RH) and ToL, only some fluctuation (Figure 6d).

https://doi.org/10.5194/acp-2022-264
Preprint. Discussion started: 19 April 2022

Atmospheric Chemistry and Physics Discussions

350

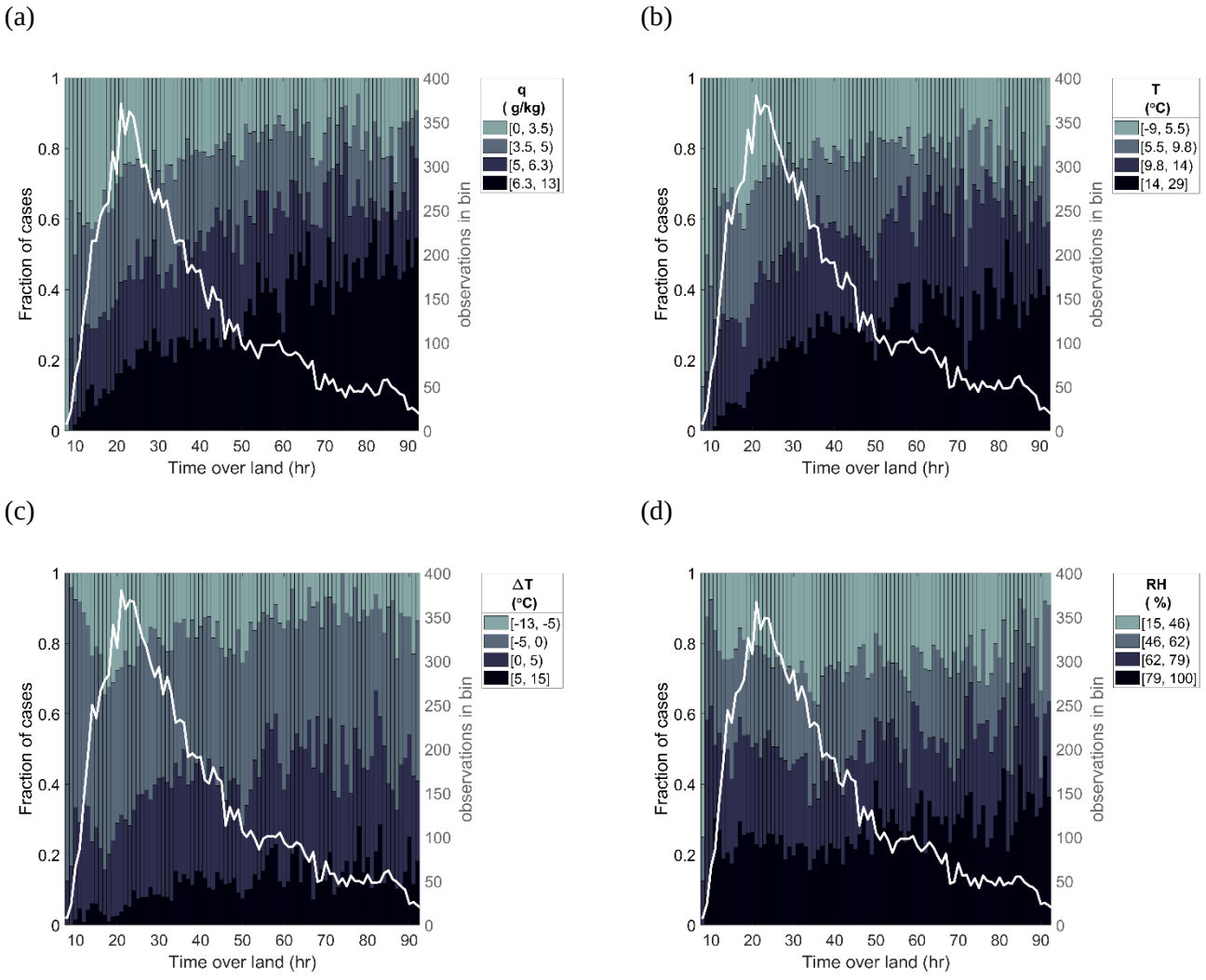

Figure 6. Fractions of observed (a) specific humidity (q), (b) temperature, (c) temperature deviation from monthly median and (d) relative humidity, in 4 different value ranges, as a function of ToL. The white lines and the right y-axes show the number of observations in each bin. The general description of this figure is the same as for Figure 3, except that here the ToLs are binned into hourly bins, and group value limits in panel (c) are predefined and not based on percentiles. The same ToL cut-off limit of 92.5 h is still maintained for consistency.

355

https://doi.org/10.5194/acp-2022-264
Preprint. Discussion started: 19 April 2022

Atmospheric Chemistry and Physics Discussions

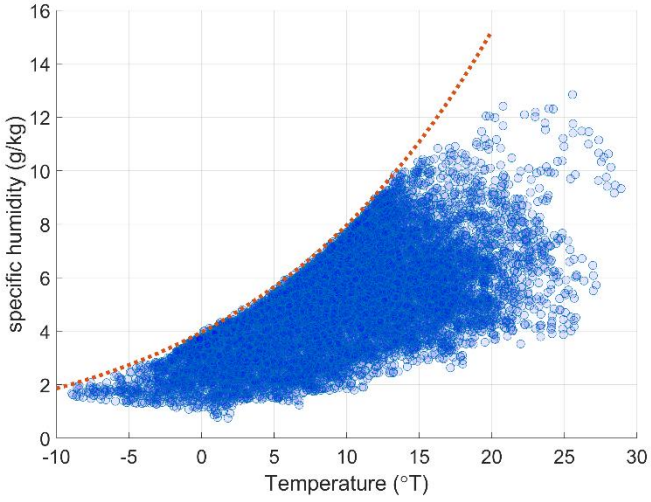

Figure 7. Observed specific humidities plotted against simultaneous observations of temperature. The red line shows the saturation specific humidity at the lowest hourly average atmospheric pressure of the observations (962 hPa).

3.3 Cloud observations as a function of Time over Land

Next, we compared satellite-based cloud observations over Hyytiälä to the air mass ToL, in order to examine potential responses in connection with the processes already observed at the surface. Previous shorter-term investigations have already suggested increases in cloud droplet number concentrations of liquid clouds as a function of ToL (Petäjä et al., 2022). Here, we investigated satellite-retrieved observations of cloud cover and optical properties in a 1° × 0.5° (latitudinal × longitudinal) sized grid enclosing the SMEAR II station. A criterion of a minimum of 20% relevant pixel coverage was also required. The data set is relatively limited, as coinciding approved satellite and clean sector trajectories are required. The number of successful daily observations also varies slightly, which may also lead to some days having better representation than others.

Median Cloud Optical Thickness (COT) within the grid is showed in Figure 8a. As the COT is estimated from 1 km × 1 km pixels that are expected to be overcast, the focus is mostly on relatively uniform cloud covers (e.g. stratus type clouds and stratocumulus). A modest increase seems to occur after ToL exceeds approximately 50 hours. Mainly the observations in the highest quartile, the COT values more than 16, become more common. However, at ToLs of approximately 80 hours or more, lower median COTs were observed again for an unknown reason, but the number of datapoints in these bins is low, making them possibly less reliable. Mean values within the 1° × 0.5° area (Figure 8 b) differ from the median values (Figure 8 a). The mean cloud optical thickness is better at capturing thicker smaller clouds that deviate more from the median of the whole grid. As a result, a patchier cloud layer with occasional thicker regions may have a much higher mean than median COT, explaining the higher mean values in Fig. 8c. Although the mean COTs are higher in value than median COTs, their behaviour as a function of ToL does not seem to differ from each other, as we see similar increases after roughly 50 hours.

https://doi.org/10.5194/acp-2022-264
Preprint. Discussion started: 19 April 2022


Atmospheric Chemistry and Physics Discussions

The lack of major differences in these trends might indicate that there is little change in the patchiness of the cloud cover with ToL; at least not enough to be observed at this resolution.

A hint of a somewhat similar phenomenon can possibly be seen in the cloud fraction (CF) (Figure 8c), where the clearest skies (median CF<0.14 and mean CF<0.24) seem to become a little less common when ToL is longer than 50 h. More than anything, there seems to be a slight drop in the prevalence of cloud fractions higher than these (i.e. median CF>0.14 and mean CF>0.24) somewhere between 35 and 50 hours but inferring any trends beyond this may not be justified, although overcast views seem also a little more common between 55 and 75 hours of ToL. The shortest ToL bin is again an exception, where cloud fraction is much higher than elsewhere, most likely again an effect associated with frontal activity.

The figures discussed above are indicative that corresponding to the effects driven by land transport onto the near-ground properties may also translate into the cloud level at relatively similar time scales. These results should, however, be considered only indicative, as the number data points is limited, making the effects somewhat uncertain. One should also remember that our data only include overcast pixels that are not separated by cloud phases, while additional uncertainties may also arise from e.g. thin clouds and sub-pixel inhomogeneities (Zhang et al., 2012). Therefore, at this point, we merely consider these as an example of possible observable effects in the cloud level, and contemplate that a future confirmation of these effects with a more detailed analysis could be beneficial.

https://doi.org/10.5194/acp-2022-264
Preprint. Discussion started: 19 April 2022

Atmospheric Chemistry and Physics Discussions

(a)

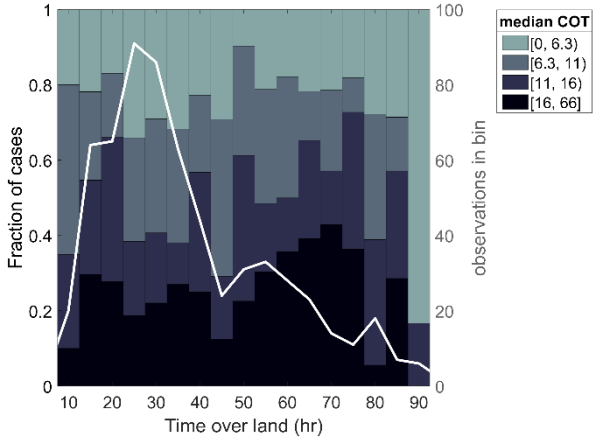

(b)

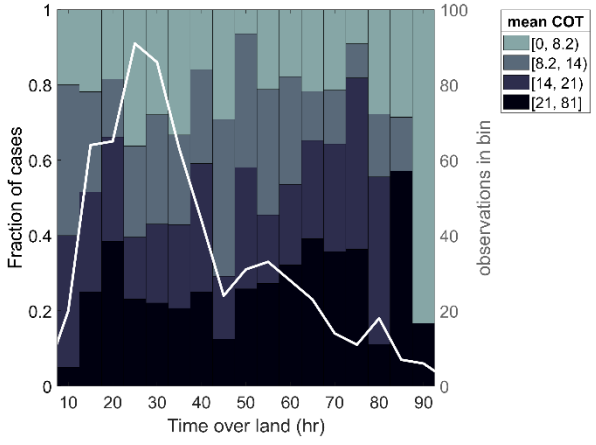

(c)

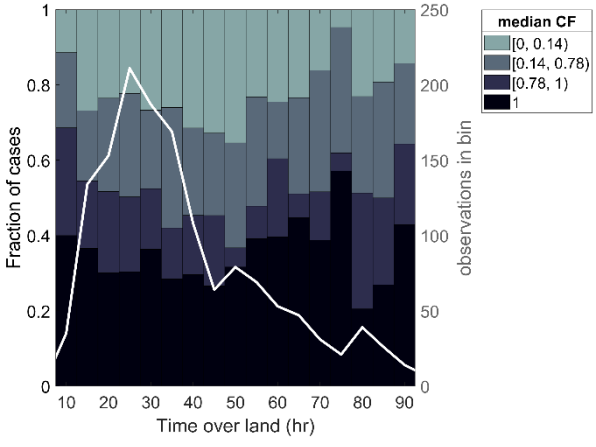

(d)

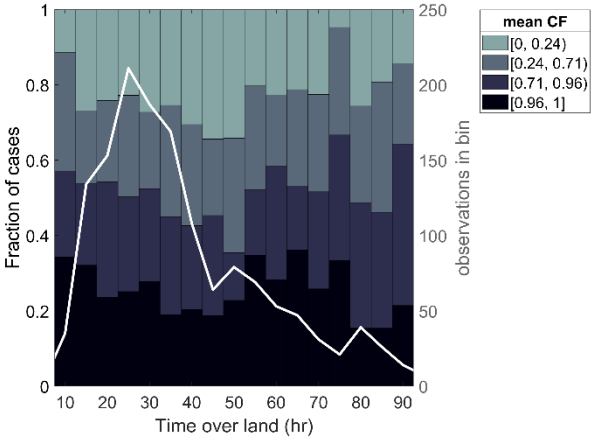

Figure 8. Fractions of satellite-observed 1°×0.5° grid (a) median COT, (b) mean COT, (c) median CF and (d) mean CF in 4 different value ranges as a function of ToL. The white lines and the right y-axes show the number of observations in each bin. The general description of this figure is the same as for Figure 3. COTs are only considered from satellite views where the number of expected overcast pixels in the 1°x0.5° area is at least 20% of the maximum observed. For CF all observations where the partial view over the area is 20% or more are accepted. Note that in (a) and (b), the two last ToL-bins have only 9 and 6 observations respectively and are therefore very unreliable.

https://doi.org/10.5194/acp-2022-264
Preprint. Discussion started: 19 April 2022

Atmospheric Chemistry and Physics Discussions

3.4 Precipitation as a function of Time over Land

Precipitation also varied with ToL. In Figure 9, the precipitation accumulation is similarly divided into value bins and their fractions are shown against the corresponding ToL. Figure 9a depicts the accumulation of longer-term precipitation from the next three hours after the arrival of the air mass. With the exception of the very short ToLs (≤12 h), with a high probability for frontal precipitation, the rain events increase in probability with an increasing ToL. This increase is modest and not strictly monotonic, while somewhat similarly to the cloud observations, the clearest increase in the precipitation probability seems to occur after a land transport time of roughly 50 hours. Any possible stabilisation seen in connection with other properties is difficult to infer here. Rather than being exclusively due to the air mass path, we cannot rule out the possibility that some of these long ToL air masses are simply moving slowly, so that the same clouds spend a longer time precipitating over the same location. The truth might be a combination of both. A drawback of investigating the 3-hour precipitation with hourly trajectories is that the rainfall (but also lack thereof) in one specific hour could be sampled up to 3 times (for 3 subsequent trajectories) if the air mass source region remained the same for an extended period. However, we also saw a similar increase in precipitation as a function of ToL in a shorter, 1-hour precipitation accumulation that is free from this issue (Figure 9b).

(a) (b)

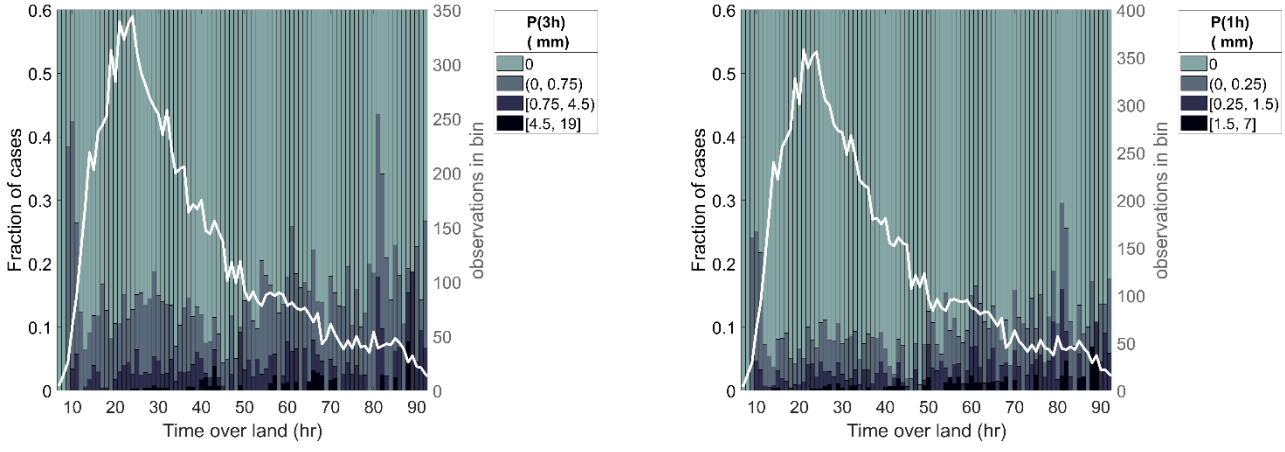

Figure 9. Fraction of rainfall in the next 3-hours (a) and 1 hour (b) in 4 different value ranges as a function of ToL of the arriving air mass. There is a break in the y-axis so that distinguishing the detail of precipitating fractions is easier. The white line shows the number of observations in each bin. Here the value groups were predefined and not based on percentiles. The rainfall value ranges are also different between the figures, the 3-hour precipitation limits being triple the 1-hour limits. One outlier was excluded from (b) (18 mm).

The increased precipitation probability with an increasing ToL is in line with the observed behaviour of both specific humidity and clouds discussed above. The evapotranspired water vapour appears to be efficiently spread into the atmospheric column, where it can condense onto cloud droplets. Figure 10 demonstrates the connection between surface-

https://doi.org/10.5194/acp-2022-264
Preprint. Discussion started: 19 April 2022

Atmospheric Chemistry and Physics Discussions

445 measured specific humidity in Hyytiälä and the CWP simultaneously measured from above, and we can see a positive correlation between the two. Similarly to other satellite-derived variables, the shown CWP is a median of a 1° × 0.5° grid, when the grid had at least 20% cloudy pixel coverage. A high CWP is seen especially in connection with specific humidities above 6 g/kg, although the scatter is also quite notable at these higher values. Such high specific humidities are more common in air masses with longer ToLs (Figure 6), so the concurrent increase in CWP can also explain the observations
450 made in COT (Figure 8).

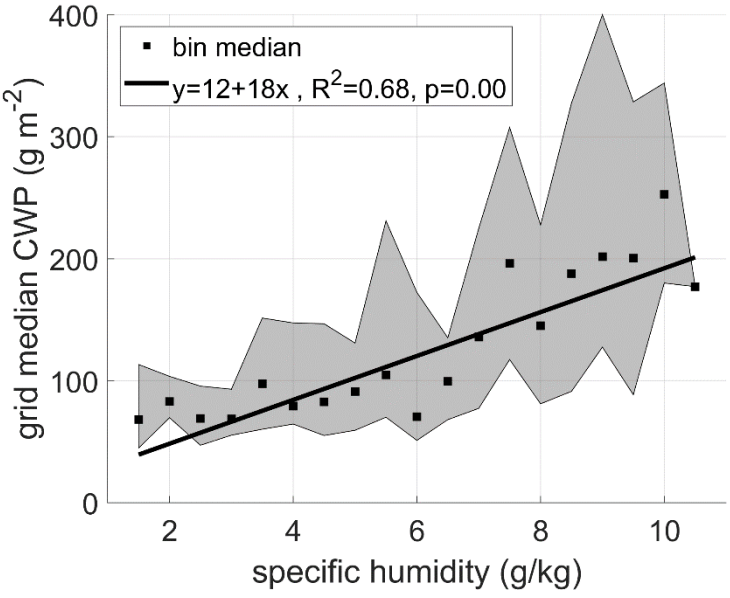

Figure 10. Cloud water path as a function of specific humidity. The squares correspond to the median of observations in each 0.5 g/kg-wide specific humidity bin, and the range between 25th and 75th percentiles is shaded. Individual satellite observations were
455 **median of CWP observations in a 1x0.5-degree view over Hyytiälä, when the cloudy pixel number was at least 20% of the maximum (i.e., same criterion as for the considered COT observations in Figure 8). A least-squares regression weighed with the number of observations in each bin is fitted to the bin median data. The regression equation, adjusted R^2 and p-value are shown in the legend.**

The moisture build-up can then eventually lead to precipitation, which we observed to increase in longer ToL air masses
460 (Figure 9). A linear trend between specific humidity and precipitation rate has been previously observed throughout northern Eurasia (Ye et al., 2015). In Figure 11, we have plotted the mean precipitation in the hour following the arrival of an air mass from our selected source region against the specific humidity measured at the station in the beginning of the same hour. This includes also non-precipitating cases, and therefore only describes the average precipitation at each specific humidity, but not the intensity of the rain events. A clear positive trend is present when specific humidity is in the range of 3 to 9 g/kg.
465 Precipitation below the "threshold value" of 3 g/kg appears to be minimal. The specific humidity of 9 g/kg seems to be highly favourable for precipitation, as the mean precipitation in the hour following these roughly 160 measurements is approximately 0.25 mm. Specific humidities higher than this are relatively few in numbers and are not associated with

https://doi.org/10.5194/acp-2022-264
Preprint. Discussion started: 19 April 2022

Atmospheric Chemistry and Physics Discussions

similarly high precipitation. It is possible that some of these high humidities were measured after the end of a rain event, or even in a fog, which could explain the high specific humidity but a lack of subsequent precipitation. When focusing on rain events specifically ("wet hours", Figure 11b) for a closer look on the intensity of the precipitation, there was also was a slight observable trend between median rainfall and specific humidity, despite the variance being large especially at higher humidities. This also suggests than rather than just being linked with more frequent precipitation, higher humidities also indicate higher precipitation rates.

(a) (b)

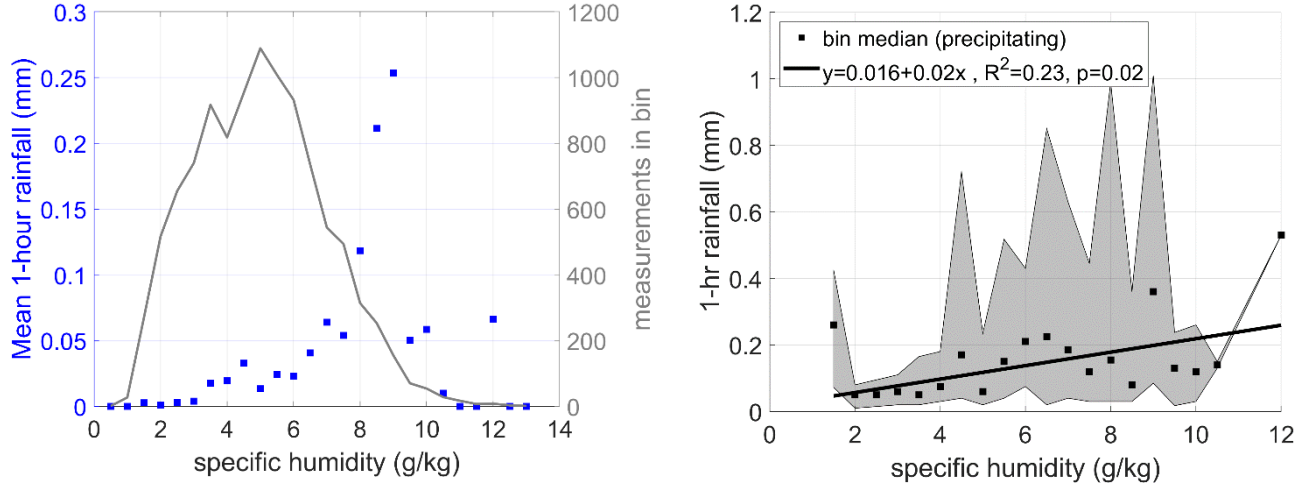

Figure 11. (a) Mean precipitation (blue squares) accumulated in an hour as a function of specific humidity measured at the beginning of the hour. The number of data points in shown again by a grey line. (b) Median precipitation accumulated in single "wet hours" as a function of specific humidity measured at the beginning of the hour. A least-squares regression weighed with the number of observations in each bin is fitted to the bin median data. The regression equation, adjusted R^2 and p-value are shown in the legend. One exceptionally high precipitation outlier was omitted from both figures.

4 Conclusions

We investigated the influences of boreal forests on clean air masses entering over the Fennoscandian land from the ocean between northern and western directions, and explored how these initially marine air masses transformed as they travelled on land. Specifically, we focused on analysing how in situ aerosol particle number size distribution, cloud condensation nuclei concentrations, humidity, cloudiness and precipitation were influenced by the interaction time between the air masses and the boreal biome. We followed the approach of Tunved et al. (2006) and (Petäjä et al., 2022), and determined a Time over Land (ToL) value for hourly air mass back trajectories within our pre-determined clean sector. Our analysis covered an extensive eight to 11 years of data, between the months of April and September, from Hyytiälä, Finland. The analysis

https://doi.org/10.5194/acp-2022-264
Preprint. Discussion started: 19 April 2022


Atmospheric Chemistry and Physics Discussions

utilised long data sets, which brings added confidence to the results and supports earlier investigations (e.g. Petäjä et al., 2022) focused on considerably shorter study periods.

Our analysis showed major differences in air mass properties with different times over land. As NPF events are common in air masses that have spent relatively short time over the forest environment (Petäjä et al., 2022) after leaving the marine environment, high number concentrations are often observed especially around 20 hours of ToL. When the air mass has experienced a longer ToL, total particle number concentrations tend to have decreased, but the existing particles have had time to grow larger in the presence of condensable vapours produced in the forest environment, meaning that significantly higher number concentrations of CCN are typically observed in such air masses.

As air masses were transformed from marine to a more continental forest air, they tended to accumulate more water vapour, likely from the evapotranspiration of the forest below. Temperature imposes an upper limit for the possible water content held by the air mass, but, as air warms as it travels over land, the warming can facilitate this observed increase in the specific humidity. Higher specific humidities at the surface were connected to higher column cloud water paths and increased precipitation, suggesting an interconnection between surface observations and cloud level, connecting our separate observations of increased humidity, cloudiness and precipitation at longer ToLs. While evapotranspiration provides the water content essential for the formation of the cloud droplets in longer ToL air masses, the concurrent production of CCN can increase the number concentration of cloud droplets and further boost the reflectance of the cloud cover (Christensen et al., 2020; Yli-Juuti et al., 2021).

Nearly all of the variables considered in this investigation appeared to reach a balanced state with the forest environment by approximately 60 hours of transport over land. Any variation at ToLs longer than this did not seem to produce notable differences between the air masses. Therefore, 60 hours can be considered as the approximate time scale over which an originally marine air mass transforms into a continental one that is in a steady state with natural particle sources and sinks in this environment. Although such a stabilisation was somewhat difficult to be confidently establish from the precipitation observations, we expect similar time scales to influence rainfall as well. (Petäjä et al., 2022) derived a relatively similar time scale, as they concluded that air masses experience changes in aerosol and cloud properties for up to 3 days of transport. Based on our analysis, approximately 60 hours seems therefore to be needed before the aerosol-cloud interactions driven by the boreal forest emissions can reach their full effect. This can be adapted to reflect the typical size of the area this would require and highlights the fact that general observations made near the edge of the boreal forest may not be generalisable over a wider region, as in many of these air masses the forest interactions might not have yet taken their full effect. This can be only expected of the air masses with ToL close to 60 hours or more, which for example in our study location was not the case for a majority of the air masses, as the median ToL of cleans sector trajectories was only 33 hours. Our investigation was also limited to tracking the airmasses over 4 days and does not account for the changes possibly later down the line.

Considering these spatial and temporal scales presented here could prove useful for estimating and/or modelling the area and strength of the associated feedbacks. The observed moisture provided by the forest, and the increase in precipitation down the line, also highlights the role of forests in inland moisture transport, important for both the stability of ecosystems as

https://doi.org/10.5194/acp-2022-264
Preprint. Discussion started: 19 April 2022


Atmospheric Chemistry and Physics Discussions

well as water security at longer distances from the coast. The processes discussed here are also worth to be considered in forestry practices, or even in potential plans of re- or afforestation.

Our analysis focused on a broad view of changes occurring in air masses as they travelled over Fennoscandian boreal forest during the growing season. These changes might look different in warmer air masses, travelling across a boreal forest with different BVOC emissions and a different evaporation rate, which may characterise the future climate. For better tools to estimate how these effects might look in the future, conducting a similar analysis with specific focuses could be beneficial, including a separation of seasons or a focus on extreme events. As our cloud data were very limited, investigating the relationship between cloud optical properties and boreal transport time with a much more detailed data would also seem like the natural next step in this type of analysis.

Code and Data availability: Derived data supporting the findings of this study are available from the corresponding author on request or through the references provided for the data in the manuscript.

Competing interests: The authors declare that they have no conflict of interest.

Author contribution: The idea and design of the study were conceived by EE, TP and MK. MR wrote the manuscript, analysed most of the data and provided the visualisations under the supervision of EE and TP, while also LS, VMK, TN and MK were involved in the interpretation. Supporting analysis or data were provided by HK and LS. All authors also contributed to the manuscript through reviewing and commenting.

Acknowledgements:

The work was supported by Atmosphere and Climate Competence Center (ACCC) Flagship funded by the Academy of Finland (grant number 337549), Center of Excellence in Atmospheric Sciences, and Academy of Finland with several projects, such as NANOBIOMASS (grant No. 307537), ACRoBEAR (grant No. 334792), and grant number 311932. The work was partially funded by European Commission via iCUPE (grant No. 689443) and FORCeS (grant No. 821205) projects. We also acknowledge the projects: “Quantifying carbon sink, CarbonSink+ and their interaction with air quality” INAR project funded by Jane and Aatos Erkko Foundation, and European Research Council (ERC) project ATM-GTP (contract No. 742206).

We gratefully acknowledge the NOAA Air Resources Laboratory (ARL) for the provision of the HYSPLIT transport and dispersion model used in this publication. We are grateful for Pasi Aalto for providing the automated trajectory calculation utilized in this work. We extend our gratitude to the SMEAR II technical staff for their maintenance work ensuring good quality data during the last decades. Raw data were generated at INAR, University of Helsinki. The MODIS/Terra and Aqua Clouds 5-Min L2 Swath 1km and 5km and MODIS Terra and Aqua MCD12C1 datasets were acquired from the Level-1 and

https://doi.org/10.5194/acp-2022-264
Preprint. Discussion started: 19 April 2022

Atmospheric Chemistry and Physics Discussions

Atmosphere Archive & Distribution System (LAADS) Distributed Active Archive Center (DAAC), located in the Goddard Space Flight Center in Greenbelt, Maryland (https://ladsweb.modaps.eosdis.nasa.gov/).

555

References

Aalto, J., Porcar-Castell, A., Atherton, J., Kolari, P., Pohja, T., Hari, P., Nikinmaa, E., Petaja, T., and Back, J.: Onset of
560 photosynthesis in spring speeds up monoterpene synthesis and leads to emission bursts, Plant Cell Environ., 38, 2299–2312, https://doi.org/10.1111/pce.12550, 2015.

Abbott, B. W., Jones, J. B., Schuur, E. A. G., Chapin, F. S., Bowden, W. B., Bret-Harte, M. S., Epstein, H. E., Flannigan, M. D., Harms, T. K., Hollingsworth, T. N., Mack, M. C., McGuire, A. D., Natali, S. M., Rocha, A. v., Tank, S. E., Turetsky, M. R., Vonk, J. E., Wickland, K. P., Aiken, G. R., Alexander, H. D., Amon, R. M. W., Benscoter, B. W., Bergeron, Y., Bishop,
565 K., Blarquez, O., Bond-Lamberty, B., Breen, A. L., Buffam, I., Cai, Y., Carcaillet, C., Carey, S. K., Chen, J. M., Chen, H. Y. H., Christensen, T. R., Cooper, L. W., Cornelissen, J. H. C., de Groot, W. J., Deluca, T. H., Dorrepaal, E., Fetcher, N., Finlay, J. C., Forbes, B. C., French, N. H. F., Gauthier, S., Girardin, M. P., Goetz, S. J., Goldammer, J. G., Gough, L., Grogan, P., Guo, L., Higuera, P. E., Hinzman, L., Hu, F. S., Hugelius, G., Jafarov, E. E., Jandt, R., Johnstone, J. F., Karlsson, J., Kasischke, E. S., Kattner, G., Kelly, R., Keuper, F., Kling, G. W., Kortelainen, P., Kouki, J., Kuhry, P., Laudon, H.,
570 Laurion, I., MacDonald, R. W., Mann, P. J., Martikainen, P. J., McClelland, J. W., Molau, U., Oberbauer, S. F., Olefeldt, D., Paré, D., Parisien, M. A., Payette, S., Peng, C., Pokrovsky, O. S., Rastetter, E. B., Raymond, P. A., Raynolds, M. K., Rein, G., Reynolds, J. F., Robards, M., Rogers, B. M., Schdel, C., Schaefer, K., Schmidt, I. K., Shvidenko, A., Sky, J., Spencer, R. G. M., Starr, G., Striegl, R. G., Teisserenc, R., Tranvik, L. J., Virtanen, T., Welker, J. M., et al.: Biomass offsets little or none of permafrost carbon release from soils, streams, and wildfire: An expert assessment, Environ. Res. Lett., 11, 034014,
575 https://doi.org/10.1088/1748-9326/11/3/034014, 2016.

Arneth, A., Makkonen, R., Olin, S., Paasonen, P., Holst, T., Kajos, M. K., Kulmala, M., Maximov, T., Miller, P. A., and Schurgers, G.: Future vegetation-climate interactions in Eastern Siberia: an assessment of the competing effects of CO2 and secondary organic aerosols, Atmos. Chem. Phys., 16, 5243–5262, https://doi.org/10.5194/acp-16-5243-2016, 2016.

Asmi, E., Kondratyev, V., Brus, D., Laurila, T., Lihavainen, H., Backman, J., Vakkari, V., Aurela, M., Hatakka, J., Viisanen,
580 Y., Uttal, T., Ivakhov, V., and Makshtas, A.: Aerosol size distribution seasonal characteristics measured in Tiksi, Russian Arctic, Atmos. Chem. Phys., 16, 1271–1287, https://doi.org/10.5194/acp-16-1271-2016, 2016.

Belward, A. S., Estes, J. E., and Kline, K. D.: The IGBP-DIS global 1-km land-cover data set DISCover: A project overview, Photogramm. Eng. Remote Sensing, 65, 1013–1020, 1999.

Betts, R. A.: Offset of the potential carbon sink from boreal forestation by decreases in surface albedo, Nature, 408, 187–190, https://doi.org/10.1038/35041545, 2000.

Birmili, W., Berresheim, H., Plass-Dülmer, C., Elste, T., Gilge, S., Wiedensohler, A., and Uhrner, U.: The Hohenpeissenberg aerosol formation experiment (HAFEX): a long-term study including size-resolved aerosol, H2SO4, OH, and monoterpenes measurements, Atmos. Chem. Phys., 3, 361–376, https://doi.org/10.5194/acp-3-361-2003, 2003.

Bonan, G. B.: Forests and climate change: Forcings, feedbacks, and the climate benefits of forests, Science, 320, 1444–1449, https://doi.org/10.1126/science.1155121, 2008.

Bosman, P. J. M., van Heerwaarden, C. C., and Teuling, A. J.: Sensible heating as a potential mechanism for enhanced cloud formation over temperate forest, Q. J. R. Meteorol. Soc., 145, 450–468, https://doi.org/https://doi.org/10.1002/qj.3441, 2019.

Broxton, P. D., Zeng, X., Sulla-Menashe, D., and Troch, P. A.: A Global Land Cover Climatology Using MODIS Data, J. Appl. Meteorol. Climatol., 53, 1593–1605, https://doi.org/10.1175/JAMC-D-13-0270.1, 2014.

Bruhwiler, L., Parmentier, F.-J. W., Crill, P., Leonard, M., and Palmer, P. I.: The Arctic Carbon Cycle and Its Response to Changing Climate, Curr. Clim. Chang. Reports, 7, 14–34, https://doi.org/10.1007/s40641-020-00169-5, 2021.

Carslaw, K. S., Boucher, O., Spracklen, D. v, Mann, G. W., Rae, J. G. L., Woodward, S., and Kulmala, M.: A review of natural aerosol interactions and feedbacks within the Earth system, Atmos. Chem. Phys., 10, 1701–1737, https://doi.org/10.5194/acp-10-1701-2010, 2010.

Christensen, M. W., Jones, W. K., and Stier, P.: Aerosols enhance cloud lifetime and brightness along the stratus-to-cumulus transition, Proc. Natl. Acad. Sci., 117, 17591 LP – 17598, https://doi.org/10.1073/pnas.1921231117, 2020.

Dal Maso, M., Kulmala, M., Riipinen, I., Wagner, R., Hussein, T., Aalto, P. P., and Lehtinen, K. E. J.: Formation and growth of fresh atmospheric aerosols: eight years of aerosol size distribution data from SMEAR II, Hyytiala, Finland, Boreal Environ. Res., 10, 323–336, 2005.

Draxler, R. and Hess, G.: An overview of the HYSPLIT_4 modeling system for trajectories, dispersion, and deposition, Aust. Meteorol. Mag., 47, 295–308, 1998.

Duveiller, G., Filipponi, F., Ceglar, A., Bojanowski, J., Alkama, R., and Cescatti, A.: Revealing the widespread potential of forests to increase low level cloud cover, Nat. Commun., 12, 4337, https://doi.org/10.1038/s41467-021-24551-5, 2021.

Ehn, M., Thornton, J. A., Kleist, E., Sipila, M., Junninen, H., Pullinen, I., Springer, M., Rubach, F., Tillmann, R., Lee, B., Lopez-Hilfiker, F., Andres, S., Acir, I.-H., Rissanen, M., Jokinen, T., Schobesberger, S., Kangasluoma, J., Kontkanen, J., Nieminen, T., Kurten, T., Nielsen, L. B., Jorgensen, S., Kjaergaard, H. G., Canagaratna, M., Dal Maso, M., Berndt, T., Petaja, T., Wahner, A., Kerminen, V.-M., Kulmala, M., Worsnop, D. R., Wildt, J., and Mentel, T. F.: A large source of low-volatility secondary organic aerosol, Nature, 506, 476–479, https://doi.org/10.1038/nature13032, 2014.

van der Ent, R. J., Savenije, H. H. G., Schaefli, B., and Steele-Dunne, S. C.: Origin and fate of atmospheric moisture over continents, Water Resour. Res., 46, W09525–W09525, https://doi.org/10.1029/2010WR009127, 2010.

European Commission, Eurostat, Agriculture, forestry and fishery statistics : 2020 edition, edited by: Cook, E., https://doi.org/doi/10.2785/496803, 2021.

Euskirchen, E. S., McGuire, A. D., Chapin ,III, F. S., and Rupp, T. S.: The changing effects of Alaska's boreal forests on the climate system, Can. J. For. Res., 40, 1336–1346, https://doi.org/10.1139/X09-209, 2010.

Friedl, M. and Sulla-Menashe, D.: MCD12C1 MODIS/Terra+Aqua Land Cover Type Yearly L3 Global 0.05Deg CMG. NASA LP DAAC., https://doi.org/10.5067/MODIS/MCD12C1.006, 2015.

Gonzalez-Eguino, M. and Neumann, M. B.: Significant implications of permafrost thawing for climate change control, Clim. Change, 136, 381–388, https://doi.org/10.1007/s10584-016-1666-5, 2016.

Hari, P. and Kulmala, M.: Station for measuring ecosystem-atmosphere relations (SMEAR II), Boreal Environ. Res., 10, 315-322, 2005.

Hari, P., Kerminen, V.-M., Kulmala, L., Kulmala, M., Noe, S., Petaja, T., Vanhatalo, A., and Back, J.: Annual cycle of Scots pine photosynthesis, Atmos. Chem. Phys., 17, 15045–15053, https://doi.org/10.5194/acp-17-15045-2017, 2017.

Hartley, I. P., Garnett, M. H., Sommerkorn, M., Hopkins, D. W., Fletcher, B. J., Sloan, V. L., Phoenix, G. K., and Wookey, P. A.: A potential loss of carbon associated with greater plant growth in the European Arctic, Nat. Clim. Chang., 2, 875–879, https://doi.org/10.1038/NCLIMATE1575, 2012.

Heikkinen, L., Äijälä, M., Riva, M., Luoma, K., Dallenbach, K., Aalto, J., Aalto, P., Aliaga, D., Aurela, M., Keskinen, H., Makkonen, U., Rantala, P., Kulmala, M., Petäjä, T., Worsnop, D., and Ehn, M.: Long-term sub-micrometer aerosol chemical composition in the boreal forest: inter- and intra-annual variability, Atmos. Chem. Phys., 20, 3151–3180, https://doi.org/10.5194/acp-20-3151-2020, 2020.

Heikkinen, L., Äijälä, M., Daellenbach, K. R., Chen, G., Garmash, O., Aliaga, D., Graeffe, F., Räty, M., Luoma, K., Aalto, P., Kulmala, M., Petäjä, T., Worsnop, D., and Ehn, M.: Eight years of sub-micrometre organic aerosol composition data from the boreal forest characterized using a machine-learning approach, Atmos. Chem. Phys., 21, 10081–10109, https://doi.org/10.5194/acp-21-10081-2021, 2021.

Hornberger, G. M., Wiberg, P. L., Raffensperger, J. P., and D'Odorico, P.: Elements of physical hydrology, Second edi., Johns Hopkins University Press, Baltimore, Md, 2014.

Hudson, J. G. and Noble, S.: CCN and Vertical Velocity Influences on Droplet Concentrations and Supersaturations in Clean and Polluted Stratus Clouds, J. Atmos. Sci., 71, 312–331, https://doi.org/10.1175/JAS-D-13-086.1, 2014.

Hyvönen, S., Junninen, H., Laakso, L., Dal Maso, M., Grönholm, T., Bonn, B., Keronen, P., Aalto, P., Hiltunen, V., Pohja, T., Launiainen, S., Hari, P., Mannila, H., and Kulmala, M.: A look at aerosol formation using data mining techniques, Atmos. Chem. Phys., 5, 3345–3356, https://doi.org/10.5194/acp-5-3345-2005, 2005.

Keenan, T. F., Prentice, I. C., Canadell, J. G., Williams, C. A., Wang, H., Raupach, M., and Collatz, G. J.: Recent pause in the growth rate of atmospheric CO2 due to enhanced terrestrial carbon uptake, Nat. Commun., 7, 13428, https://doi.org/10.1038/ncomms13428, 2016.

Kerminen, V.-M., Paramonov, M., Anttila, T., Riipinen, I., Fountoukis, C., Korhonen, H., Asmi, E., Laakso, L., Lihavainen, H., Swietlicki, E., Svenningsson, B., Asmi, A., Pandis, S. N., Kulmala, M., and Petaja, T.: Cloud condensation nuclei

production associated with atmospheric nucleation: a synthesis based on existing literature and new results, Atmos. Chem. Phys., 12, 12037–12059, https://doi.org/10.5194/acp-12-12037-2012, 2012.

Kozii, N., Haahti, K., Tor-ngern, P., Chi, J., Hasselquist, E. M., Laudon, H., Launiainen, S., Oren, R., Peichl, M., Wallerman, J., and Hasselquist, N. J.: Partitioning growing season water balance within a forested boreal catchment using sap flux, eddy covariance, and a process-based model, Hydrol. Earth Syst. Sci., 24, 2999–3014, https://doi.org/10.5194/hess-24-2999-2020, 2020.

Kulmala, M., Suni, T., Lehtinen, K. E. J., Dal Maso, M., Boy, M., Reissell, A., Rannik, Ü., Aalto, P., Keronen, P., Hakola, H., Bäck, J., Hoffmann, T., Vesala, T., and Hari, P.: A new feedback mechanism linking forests, aerosols, and climate, Atmos. Chem. Phys., 4, 557–562, https://doi.org/10.5194/acp-4-557-2004, 2004.

Kulmala, M., Nieminen, T., Nikandrova, A., Lehtipalo, K., Manninen, H. E., Kajos, M. K., Kolari, P., Lauri, A., Petaja, T., Krejci, R., Hansson, H.-C., Swietlicki, E., Lindroth, A., Christensen, T. R., Arneth, A., Hari, P., Back, J., Vesala, T., and Kerminen, V.-M.: CO2-induced terrestrial climate feedback mechanism: From carbon sink to aerosol source and back, Boreal Environ. Res, 19, 122–131, 2014.

Kulmala, M., Kerminen, V.-M., Petäjä, T., Ding, A. J., and Wang, L.: Atmospheric gas-to-particle conversion: why NPF events are observed in megacities?, Faraday Discuss., 200, 271–288, https://doi.org/10.1039/C6FD00257A, 2017.

Kulmala, M., Ezhova, E., Kalliokoski, T., Noe, S., Vesala, T., Lohila, A., Liski, J., Makkonen, R., Bäck, J., Petäjä, T., and others: CarbonSink+--Accounting for multiple climate feedbacks from forests, Boreal Environ. Res., 25, 145–159, 2020.

Kulmala, M., Dada, L., Daellenbach, K. R., Yan, C., Stolzenburg, D., Kontkanen, J., Ezhova, E., Hakala, S., Tuovinen, S., Kokkonen, T. v, Kurppa, M., Cai, R., Zhou, Y., Yin, R., Baalbaki, R., Chan, T., Chu, B., Deng, C., Fu, Y., Ge, M., He, H., Heikkinen, L., Junninen, H., Liu, Y., Lu, Y., Nie, W., Rusanen, A., Vakkari, V., Wang, Y., Yang, G., Yao, L., Zheng, J., Kujansuu, J., Kangasluoma, J., Petäjä, T., Paasonen, P., Järvi, L., Worsnop, D., Ding, A., Liu, Y., Wang, L., Jiang, J., Bianchi, F., and Kerminen, V.-M.: Is reducing new particle formation a plausible solution to mitigate particulate air pollution in Beijing and other Chinese megacities?, Faraday Discuss., 226, 334–347, https://doi.org/10.1039/D0FD00078G, 2021.

Lappalainen, H. K., Sevanto, S., Bäck, J., Ruuskanen, T. M., Kolari, P., Taipale, R., Rinne, J., Kulmala, M., and Hari, P.: Day-time concentrations of biogenic volatile organic compounds in a boreal forest canopy and their relation to environmental and biological factors, Atmos. Chem. Phys., 9, 5447–5459, https://doi.org/10.5194/acp-9-5447-2009, 2009.

Liao, L., Kerminen, V.-M., Boy, M., Kulmala, M., and Dal Maso, M.: Temperature influence on the natural aerosol budget over boreal forests, Atmos. Chem. Phys., 14, 8295–8308, https://doi.org/10.5194/acp-14-8295-2014, 2014.

Loreto, F. and Schnitzler, J.-P.: Abiotic stresses and induced BVOCs, Trends Plant Sci., 15, 154–166, https://doi.org/https://doi.org/10.1016/j.tplants.2009.12.006, 2010.

Loveland, T. R. and Belward, A. S.: The International Geosphere Biosphere Programme Data and Information System global land cover data set (DISCover), Acta Astronaut., 41, 681–689, https://doi.org/https://doi.org/10.1016/S0094-5765(98)00050-2, 1997.

Mäkelä, J. M., Aalto, P., Jokinen, V., Pohja, T., Nissinen, A., Palmroth, S., Markkanen, T., Seitsonen, K., Lihavainen, H., and Kulmala, M.: Observations of ultrafine aerosol particle formation and growth in boreal forest, Geophys. Res. Lett., 24, 1219–1222, https://doi.org/10.1029/97GL00920, 1997.

Nieminen, T., Asmi, A., Dal Maso, M., Aalto, P. P., Keronen, P., Petaja, T., Kulmala, M., and Kerminen, V.-M.: Trends in atmospheric new-particle formation: 16 years of observations in a boreal-forest environment, Boreal Environ. Res., 19, 191–214, 2014.

Paasonen, P., Asmi, A., Petaja, T., Kajos, M. K., Aijala, M., Junninen, H., Holst, T., Abbatt, J. P. D., Arneth, A., Birmili, W., van der Gon, H. D., Hamed, A., Hoffer, A., Laakso, L., Laaksonen, A., Leaitch, W. R., Plass-Duelmer, C., Pryor, S. C., Raisanen, P., Swietlicki, E., Wiedensohler, A., Worsnop, D. R., Kerminen, V.-M., and Kulmala, M.: Warming-induced increase in aerosol number concentration likely to moderate climate change, Nat. Geosci., 6, 438–442, https://doi.org/10.1038/NGEO1800, 2013.

Paasonen, P., Peltola, M., Kontkanen, J., Junninen, H., Kerminen, V.-M., and Kulmala, M.: Comprehensive analysis of particle growth rates from nucleation mode to cloud condensation nuclei in boreal forest, Atmos. Chem. Phys., 18, 12085–12103, https://doi.org/10.5194/acp-18-12085-2018, 2018.

Paramonov, M., Aalto, P. P., Asmi, A., Prisle, N., Kerminen, V.-M., Kulmala, M., and Petaja, T.: The analysis of size-segregated cloud condensation nuclei counter (CCNC) data and its implications for cloud droplet activation, Atmos. Chem. Phys., 13, 10285–10301, https://doi.org/10.5194/acp-13-10285-2013, 2013.

Paramonov, M., Kerminen, V.-M., Gysel, M., Aalto, P. P., Andreae, M. O., Asmi, E., Baltensperger, U., Bougiatioti, A., Brus, D., Frank, G. P., Good, N., Gunthe, S. S., Hao, L., Irwin, M., Jaatinen, A., Juranyi, Z., King, S. M., Kortelainen, A., Kristensson, A., Lihavainen, H., Kulmala, M., Lohmann, U., Martin, S. T., McFiggans, G., Mihalopoulos, N., Nenes, A., O'Dowd, C. D., Ovadnevaite, J., Petaja, T., Poschl, U., Roberts, G. C., Rose, D., Svenningsson, B., Swietlicki, E., Weingartner, E., Whitehead, J., Wiedensohler, A., Wittbom, C., and Sierau, B.: A synthesis of cloud condensation nuclei counter (CCNC) measurements within the EUCAARI network, Atmos. Chem. Phys., 15, 12211–12229, https://doi.org/10.5194/acp-15-12211-2015, 2015.

Pearson, R. G., Phillips, S. J., Loranty, M. M., Beck, P. S. A., Damoulas, T., Knight, S. J., and Goetz, S. J.: Shifts in Arctic vegetation and associated feedbacks under climate change, Nat. Clim. Chang., 3, 673–677, https://doi.org/10.1038/NCLIMATE1858, 2013.

Peñuelas, J. and Staudt, M.: BVOCs and global change, Trends Plant Sci., 15, 133–144, https://doi.org/10.1016/J.TPLANTS.2009.12.005, 2010.

Petäjä, T., Tabakova, K., Manninen, A., Ezhova, E., O'Connor, E., Moisseev, D., Sinclair, V. A., Backman, J., Levula, J., Luoma, K., Virkkula, A., Paramonov, M., Räty, M., Äijälä, M., Heikkinen, L., Ehn, M., Sipilä, M., Yli-Juuti, T., Virtanen, A., Ritsche, M., Hickmon, N., Pulik, G., Rosenfeld, D., Worsnop, D. R., Bäck, J., Kulmala, M., and Kerminen, V.-M.: Influence of biogenic emissions from boreal forests on aerosol–cloud interactions, Nat. Geosci., 15, 42–47, https://doi.org/10.1038/s41561-021-00876-0, 2022.

Pinsky, M., Mazin, I. P., Korolev, A., and Khain, A.: Supersaturation and diffusional droplet growth in liquid clouds: Polydisperse spectra, J. Geophys. Res. Atmos., 119, 12,812-872,887, https://doi.org/https://doi.org/10.1002/2014JD021885, 2014.

Platnick, S., Ackerman, S., King, M., Wind, G., Meyer, K., Menzel, P., Frey, R., Holz, R., Baum, B., and Yang, P.: MODIS atmosphere L2 cloud product (06_L2), http://dx.doi.org/10.5067/MODIS/MOD06_L2.061, http://dx.doi.org/10.5067/MODIS/MYD06_L2.061, 2017.

Platnick, S., Meyer, K. g., King, M. d., Wind, G., Amarasinghe, N., Marchant, B., Arnold, G. T., Zhang, Z., Hubanks, P. A., Ridgway, B., and Riedi, J.: MODIS Cloud Optical Properties: User Guide for the Collection 6/6.1 Level-2 MOD06/MYD06 Product and Associated Level-3 Datasets, version 1.1, 2018.

Prăvălie, R.: Major perturbations in the Earth's forest ecosystems. Possible implications for global warming, Earth-Science Rev., 185, 544–571, https://doi.org/10.1016/j.earscirev.2018.06.010, 2018.

Pruppacher, H. R. and Klett, J. D.: Microphysics of Clouds and Precipitation, 2. Aufl., Springer Science + Business Media, 2010.

Qian, H., Joseph, R., and Zeng, N.: Enhanced terrestrial carbon uptake in the Northern High Latitudes in the 21st century from the Coupled Carbon Cycle Climate Model Intercomparison Project model projections, Glob. Chang. Biol., 16, 641–656, https://doi.org/10.1111/j.1365-2486.2009.01989.x, 2010.

Rantala, P., Aalto, J., Taipale, R., Ruuskanen, T. M., and Rinne, J.: Annual cycle of volatile organic compound exchange between a boreal pine forest and the atmosphere, Biogeosciences, 12, 5753–5770, https://doi.org/10.5194/bg-12-5753-2015, 2015.

Roberts, G. C. and Nenes, A.: A continuous-flow streamwise thermal-gradient CCN chamber for atmospheric measurements, Aerosol Sci. Technol., 39, 206–221, https://doi.org/10.1080/027868290913988, 2005.

Rose, D., Gunthe, S. S., Mikhailov, E., Frank, G. P., Dusek, U., Andreae, M. O., and Poeschl, U.: Calibration and measurement uncertainties of a continuous-flow cloud condensation nuclei counter (DMT-CCNC): CCN activation of ammonium sulfate and sodium chloride aerosol particles in theory and experiment, Atmos. Chem. Phys., 8, 1153–1179, https://doi.org/10.5194/acp-8-1153-2008, 2008.

Schmale, J., Henning, S., Henzing, B., Keskinen, H., Sellegri, K., Ovadnevaite, J., Bougiatioti, A., Kalivitis, N., Stavroulas, I., Jefferson, A., Park, M., Schlag, P., Kristensson, A., Iwamoto, Y., Pringle, K., Reddington, C., Aalto, P., Äijälä, M., Baltensperger, U., Bialek, J., Birmili, W., Bukowiecki, N., Ehn, M., Fjæraa, A. M., Fiebig, M., Frank, G., Fröhlich, R., Frumau, A., Furuya, M., Hammer, E., Heikkinen, L., Herrmann, E., Holzinger, R., Hyono, H., Kanakidou, M., Kiendler-Scharr, A., Kinouchi, K., Kos, G., Kulmala, M., Mihalopoulos, N., Motos, G., Nenes, A., O'Dowd, C., Paramonov, M., Petäjä, T., Picard, D., Poulain, L., Prévôt, A. S. H., Slowik, J., Sonntag, A., Swietlicki, E., Svenningsson, B., Tsurumaru, H., Wiedensohler, A., Wittbom, C., Ogren, J. A., Matsuki, A., Yum, S. S., Myhre, C. L., Carslaw, K., Stratmann, F., and Gysel, M.: Collocated observations of cloud condensation nuclei, particle size distributions, and chemical composition, Sci. Data, 4, 170003, https://doi.org/10.1038/sdata.2017.3, 2017.

Schneider, U., Finger, P., Meyer-Christoffer, A., Rustemeier, E., Ziese, M., and Becker, A.: Evaluating the Hydrological Cycle over Land Using the Newly-Corrected Precipitation Climatology from the Global Precipitation Climatology Centre (GPCC), Atmos., https://doi.org/10.3390/atmos8030052, 2017.

Schuur, E. A. G., Vogel, J. G., Crummer, K. G., Lee, H., Sickman, J. O., and Osterkamp, T. E.: The effect of permafrost thaw on old carbon release and net carbon exchange from tundra, Nature, 459, 556–559, https://doi.org/10.1038/nature08031, 2009.

Scott, C. E., Rap, A., Spracklen, D. v., Forster, P. M., Carslaw, K. S., Mann, G. W., Pringle, K. J., Kivekäs, N., Kulmala, M., Lihavainen, H., and Tunved, P.: The direct and indirect radiative effects of biogenic secondary organic aerosol, Atmos. Chem. Phys., 14, 447–470, https://doi.org/10.5194/acp-14-447-2014, 2014.

Serreze, M. C. and Barry, R. G.: Processes and impacts of Arctic amplification: A research synthesis, Glob. Planet. Change, 77, 85–96, https://doi.org/10.1016/j.gloplacha.2011.03.004, 2011.

Sogacheva, L., Dal Maso, M., Kerminen, V. M., and Kulmala, M.: Probability of nucleation events and aerosol particle concentration in different air mass types arriving at Hyytiala southern Finland, based on back trajectories analysis, Boreal Environ. Res., 10, 479–491, 2005.

Sporre, M. K., Blichner, S. M., Karset, I. H. H., Makkonen, R., and Berntsen, T. K.: BVOC–aerosol–climate feedbacks investigated using NorESM, Atmos. Chem. Phys., 19, 4763–4782, https://doi.org/10.5194/acp-19-4763-2019, 2019.

Spracklen, D. v, Bonn, B., and Carslaw, K. S.: Boreal forests, aerosols and the impacts on clouds and climate, Philos. Trans. R. Soc. A-Mathematical Phys. Eng. Sci., 366, 4613–4626, https://doi.org/10.1098/rsta.2008.0201, 2008.

Stein, A. F., Draxler, R. R., Rolph, G. D., Stunder, B. J. B., Cohen, M. D., and Ngan, F.: Noaa's Hysplit Atmospheric Transport and Dispersion Modeling System, Bull. Am. Meteorol. Soc., 96, 2059–2077, https://doi.org/10.1175/BAMS-D-14-00110.1, 2015.

Stohl, A.: Computation, accuracy and applications of trajectories - A review and bibliography, Atmos. Environ., 32, 947–966, https://doi.org/10.1016/S1352-2310(97)00457-3, 1998.

Taipale, D., Kerminen, V.-M., Ehn, M., Kulmala, M., and Niinemets, Ü.: Modelling the influence of biotic plant stress on atmospheric aerosol particle processes throughout a growing season, Atmos. Chem. Phys., 21, 17389–17431, https://doi.org/10.5194/acp-21-17389-2021, 2021.

Tarvainen, V., Hakola, H., Rinne, J., Hellen, H., and Haapanala, S.: Towards a comprehensive emission inventory of terpenoids from boreal ecosystems, Tellus Ser. B-Chemical Phys. Meteorol., 59, 526–534, https://doi.org/10.1111/j.1600-0889.2007.00263.x, 2007.

Teuling, A. J., Taylor, C. M., Meirink, J. F., Melsen, L. A., Miralles, D. G., van Heerwaarden, C. C., Vautard, R., Stegehuis, A. I., Nabuurs, G.-J., and de Arellano, J. V.-G.: Observational evidence for cloud cover enhancement over western European forests, Nat. Commun., 8, 14065, https://doi.org/10.1038/ncomms14065, 2017.

Tingey, D. T., Manning, M., Grothaus, L. C., and Burns, W. F.: Influence of Light and Temperature on Monoterpene Emission Rates from Slash Pine, Plant Physiol., 65, 797–801, https://doi.org/10.1104/pp.65.5.797, 1980.

Tunved, P., Hansson, H. C., Kerminen, V. M., Strom, J., Dal Maso, M., Lihavainen, H., Viisanen, Y., Aalto, P. P., Komppula, M., and Kulmala, M.: High natural aerosol loading over boreal forests, Science, 312, 261–263, https://doi.org/10.1126/science.1123052, 2006.

Twomey, S.: Influence of Pollution on Shortwave Albedo of Clouds, J. Atmos. Sci., 34, 1149–1152, 1977.

Väisänen, O., Ruuskanen, A., Ylisirniö, A., Miettinen, P., Portin, H., Hao, L., Leskinen, A., Komppula, M., Romakkaniemi, S., Lehtinen, K. E. J., and Virtanen, A.: In-cloud measurements highlight the role of aerosol hygroscopicity in cloud droplet formation, Atmos. Chem. Phys., 16, 10385–10398, https://doi.org/10.5194/acp-16-10385-2016, 2016.

Wild, M., Folini, D., Hakuba, M. Z., Schaer, C., Seneviratne, S. I., Kato, S., Rutan, D., Ammann, C., Wood, E. F., and Koenig-Langlo, G.: The energy balance over land and oceans: an assessment based on direct observations and CMIP5 climate models, Clim. Change, 44, 3393–3429, https://doi.org/10.1007/s00382-014-2430-z, 2015.

WMO: Guide to Instruments and Methods of Observation, Volume I - Measurement of Meteorological Variables, 2018 edition, https://library.wmo.int/index.php?id=12407&lvl=notice_display#.YiEKZd-xVEY, 2018.

Xu, R., Li, Y., Teuling, A. J., Zhao, L., Spracklen, D. v, Garcia-Carreras, L., Meier, R., Chen, L., Zheng, Y., Lin, H., and Fu, B.: Contrasting impacts of forests on cloud cover based on satellite observations, Nat. Commun., 13, 670, https://doi.org/10.1038/s41467-022-28161-7, 2022.

Ye, H., Fetzer, E. J., Wong, S., Behrangi, A., Yang, D., and Lambrigtson, B. H.: Increasing atmospheric water vapor and higher daily precipitation intensity over northern Eurasia, Geophys. Res. Lett., 42, 9404–9410, https://doi.org/10.1002/2015GL066104, 2015.

Yli-Juuti, T., Mielonen, T., Heikkinen, L., Arola, A., Ehn, M., Isokääntä, S., Keskinen, H.-M., Kulmala, M., Laakso, A., Lipponen, A., Luoma, K., Mikkonen, S., Nieminen, T., Paasonen, P., Petäjä, T., Romakkaniemi, S., Tonttila, J., Kokkola, H., and Virtanen, A.: Significance of the organic aerosol driven climate feedback in the boreal area, Nat. Commun., 12, 5637, https://doi.org/10.1038/s41467-021-25850-7, 2021.

Zhang, Q., Jia, S., Yang, L., Krishnan, P., Zhou, S., Shao, M., and Wang, X.: New particle formation (NPF) events in China urban clusters given by sever composite pollution background, Chemosphere, 262, 127842, https://doi.org/10.1016/j.chemosphere.2020.127842, 2021.

Zhang, W., Miller, P. A., Smith, B., Wania, R., Koenigk, T., and Doscher, R.: Tundra shrubification and tree-line advance amplify arctic climate warming: results from an individual-based dynamic vegetation model, Environ. Res. Lett., 8, 34023, https://doi.org/10.1088/1748-9326/8/3/034023, 2013.

Zhang, Z., Ackerman, A. S., Feingold, G., Platnick, S., Pincus, R., and Xue, H.: Effects of cloud horizontal inhomogeneity and drizzle on remote sensing of cloud droplet effective radius: Case studies based on large-eddy simulations, J. Geophys. Res. Atmos., 117, https://doi.org/https://doi.org/10.1029/2012JD017655, 2012.